Separation & Purification Reviews
Publication details, including instructions for authors and subscription information:
http://www.informaworld.com/smpp/title~content=t713597294

A Theoretical and Experimental Study of Counteracting Chromatographic Electrophoresis

Bruce R. Locke[a]; Ruben G. Carbonell[a]
[a] Department of Chemical Engineering, North Carolina State University, Raleigh, NC

To cite this Article Locke, Bruce R. and Carbonell, Ruben G.(1989) 'A Theoretical and Experimental Study of Counteracting Chromatographic Electrophoresis', Separation & Purification Reviews, 18: 1, 1 — 64
To link to this Article: DOI: 10.1080/03602548908050919
URL: http://dx.doi.org/10.1080/03602548908050919

SEPARATION AND PURIFICATION METHODS, 18(1), 1-64 (1989)

A THEORETICAL AND EXPERIMENTAL STUDY OF COUNTERACTING CHROMATOGRAPHIC ELECTROPHORESIS

Bruce R. Locke and Ruben G. Carbonell
Department of Chemical Engineering
North Carolina State University
Raleigh, NC 27695-7905

ABSTRACT

Counteracting chromatographic electrophoresis (CACE) is a separation process that combines gel chromatography with electrophoresis. This process, originally developed by O'Farrell[1], may be used for protein separation by causing a specific protein to accumulate at the interface between two bed packings of different internal porosity. In this paper a theoretical model for CACE has been developed. This model gives an accumulation criterion that specifies the operating conditions (i.e. applied field and flow rates), and the bed and protein parameters (i.e. external bed porosity, internal particle porosity, protein free mobility, and the ratio of the protein mobility in the gel to that in free solution) that lead to accumulation in the column. This accumulation criterion was tested with experimental data for the accumulation of the colored proteins ferritin, myoglobin, and cytochrome-c. This data fit the criterion fairly well for all three proteins. The theoretical model was extended to consider the transient accumulation at the interface between the packings in the column for the batch process where no product was removed from the interface, and for the continuous process where product was continuously removed from this interface. A critical value of the operating parameter $|\mu|$ (i.e. the ratio of the electrical migration to the convective flow) was found to give the fastest approach to steady-state for the continuous process.

INTRODUCTION

Counteracting chromatographic electrophoresis (CACE) is a separation process recently developed by O'Farrell[1,2,3] that combines electrophoresis with gel chromatography. Figure 1, a schematic presentation of O'Farrell's process, shows that the first half of a small diameter column was loaded with particles made of polyacrylamide gel while the second half was loaded with agarose gel particles. An electric field was applied parallel to the convective flow through the column. Since the polyacrylamide gel has a more tightly-closed pore structure than the agarose, some proteins can diffuse through the agarose gel particles but they are not able to penetrate the polyacrylamide particles. The diffusion of the protein into the agarose particles reduces the transport by convection, but does little to affect the electrical ion flux. Under suitable operating conditions of applied potential and volumetric flow, this decrease in the velocity of a particular protein leads to net fluxes which transport the protein in the direction of the interface between the two packing materials. The protein can then be accumulated at the interface. Other proteins that do not have the right molecular dimensions to penetrate the packing, the proper charge, or the proper ionic mobility will not accumulate in the column. Thus, a significant separation and purification may result. O'Farrell pointed out that there is the possibility of operating the column under steady-state conditions if the accumulated protein is continually removed from the interface. Even though O'Farrell used proteins in his experiments, it is clear that other charged molecules may also be separated using this principle.

There is a need for continuous protein separation processes that can attain high resolution and at the same time provide high concentration products. Although there are many powerful analytical electrophoresis techniques available, there are very few preparative and continuous electrophoretic methods. Mosher et al[4] have reviewed the current status of preparative electrophoresis for the separation of biological molecules. One of the prelimary limitations to the scale-up of electrophoresis processes is the generation of heat due to current flow. This heating causes convective mixing which reduces resolution. The use of continuous gel media has not only alleviated the convective mixing due to thermal effects, but it has allowed for increased resolution due to the effects of molecular size and shape on electrophoretic transport. However, this increase in resolution comes at the expense of lower throughput. Alternatives to gel media that allow for higher throughput include flow stabilization by rotation[5], and the application of a magnetic field[6]. The largest scale electrophoresis process, marketed by John Brown Engineers, is a free solution method with flow stabilized by a rotating annular

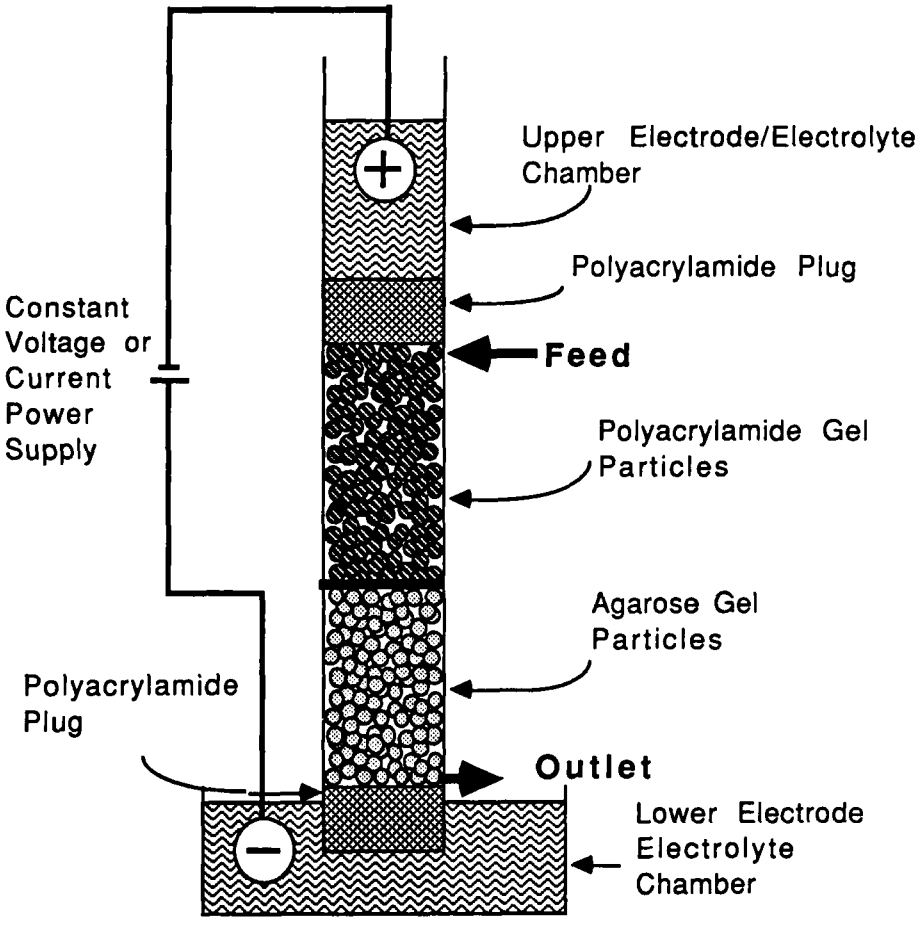

FIGURE 1
Schematic of O'Farrell's Process

column. It can have throughputs of up to 150 grams of protein per hour with fairly good resolution[4].

The CACE process is of interest both because of its potential as a continuous process, and because of the potentially high resolution that may arise from the effects of gel sieving. It is the use of gel particles rather than a continuous gel matrix that allows continuous flows with higher throughput. Since the protein is

accumulated at a pH different from its isoelectric point, the solubility, and hence final product concentration, may be higher than that usually achievable in isoelectric focusing. Finally, accumulation occurs at a predictable, and therefore controllable, location. This would be of use for the column operation and design when a product is continuously withdrawn from a side stream.

In this paper a theoretical model for CACE will be developed. A mass balance is written for each species considering the case of one-dimensional flow in the column. Species transport is assumed to occur by convective transport and electrical migration in the bulk solution, and by electrical migration alone in the pores of the particles. Mass transfer and axial dispersion are ignored. Reversible adsorption to the gel is included in the analysis, and the column is assumed to be isothermal. Electroneutrality in the bulk fluid and within the pores of the particles is assumed. Because the buffer species have a concentration and mobility very much higher than the proteins, and because they diffuse easily throughout the entire column, it is possible to assume that the conductivity in the column is constant. Since the internal porosity of the particles, the ratio of the protein mobility in the particles to that in the gel, and the adsorption constant change from the polyacrylamide side of the column to the agarose side of the column, it is necessary to consider an axial variation in these properties. This axial variation is expected to occur over the small region where the packing changes from 100% polyacrylamide to 100% agarose. In the sections that follow a criterion is developed for predicting the conditions under which protein should accumulate at this interfacial region. This accumulation criterion is given by equation (26). This criteron is then compared with experimental data taken in our laboratory.

In order to investigate the transient accumulation at the interface an averaging procedure is used. This procedure involves defining an averaging region at the interface between the two packings, and writing a mass balance over this region. Solution of this mass balance, coupled with the two mass balances that describe each side of the interfacial region, gives the transient protein accumulation in the interfacial averaging region. Equations (56) to (64) summarize the results. Although we neglect mass transfer resistance and axial dispersion in our analysis it is clear from our experimental work that they are of importance. However, neither effect will change the accumulation criterion, although they will change the concentration and rate of accumulation at the interface. In addition, reversible adsorption of the protein to the gel is found in our theoretical analysis not to affect the conditions for protein accumulation, although it does affect the concentrations of protein accumulated.

McCoy[7], Ivory[8], and Hunter[9] have developed theoretical models for CACE. McCoy[7] considered three aspects of the problem; 1) he used the method of characteristics for the case without axial dispersion, however he did not define the electrophoretic velocity in terms of the potential field and the electrophoretic mobility, and he did not include the variation of the ratio of the electrophoretic mobility in the gel to that in free solution, 2) he used the method of moments to determine the band spreading due to diffusion at the interface and 3) he used the method of characteristics for the case with a continuous variation of porosity, however he illustrated this with a linear variation of the bed porosity rather than the internal porosity of the particles. Ivory[8] considered the constant withdrawal steady-state case with axial dispersion and mass transfer resistance. He has presented some experimental results, although he did not compare the experimental observations to the predictions of the theory. Hunter[9] developed a steady-state model for the accumulation zone in analogy with isotachophoresis. In her analysis all the protein is located in the accumulation zone and only water and buffer are located in the adjacent bed regions. She used flux equations at the upper and lower boundaries of the accumulation zone coupled with the electroneutrality constraint and the expression for the electrical current in terms of concentration and species velocity to determine the protein concentration. Using the accumulation data of O'Farrell[1] she found concentrations of about an order of magnitude less than those found experimentally by O'Farrell. However, as will be discussed further, we were not able to repeat accumulation under the conditions specified by O'Farrell, and thus O'Farrell's data may not represent an adequate test of her model.

THEORETICAL DEVELOPMENT

The packing in the column is assumed to have an external void fraction ε through which the solvent moves. Some proteins, and all the small ions in the buffer, can diffuse into the solid particles. If a given ion is found in small concentration relative to the solvent, its continuity equation at any point in the fluid can be written as

$$\frac{\partial c_{i\beta}}{\partial t} + \nabla \cdot c_{i\beta} v_\beta = - \nabla \cdot J^*_{i\beta} \qquad (1)$$

where $c_{i\beta}$ is the molar concentration in the solvent or β phase, v_β is the local fluid velocity and $J_{i\beta}$* is the molar diffusive and electrophoretic flux. Using the method of spatial averaging[10], one can derive an equation for the average concentration of solute in the fluid in a region containing many particles,

$$\varepsilon \frac{\partial \langle c_{i\beta} \rangle^{\beta}}{\partial t} + \nabla \cdot \varepsilon \langle c_{i\beta} \rangle^{\beta} \langle v_{\beta} \rangle^{\beta} = - \nabla \cdot \langle J^{*}_{i\beta} \rangle^{\beta} \tag{2}$$

$$- \frac{1}{V} \int_{A_{\beta\sigma}} \mathbf{n}_{\beta\sigma} \cdot \mathbf{J}^{*}_{i\beta} \, dA$$

Here $\langle c_{i\beta} \rangle^{\beta}$ and $\langle v_{\beta} \rangle^{\beta}$ represent the interstitial concentration and fluid velocity, while $\langle J_{i\beta}^{*} \rangle^{\beta}$ represents the phase-averaged molar diffusive flux. The last term represents the rate of transport of species *i* from the fluid into the solid phase per unit volume of bed. In the equation above we have neglected hydrodynamic dispersion effects. For the flow rates and particle sizes used in our experimental work, the Peclet numbers based on the particle diameter are of the order 10^2. This suggests that axial dispersion may not be completely neglected. The main contributor to the phase-averaged diffusive flux will be the electrical field. This can be approximated by

$$- \langle J^{*}_{i\beta} \rangle^{\beta} = + \varepsilon u_{i\beta} \langle c_{i\beta} \rangle^{\beta} F \nabla \Psi \tag{3}$$

where $u_{i\beta}$is the effective mean ionic mobility of species *i* in the fluid phase, while Ψ is the mean electric potential. Appendix A gives a derivation for this flux expression, and for the flux in the solid σ phase, that relies on the assumption that the current is carried predominantly by the small buffer species that can fully penetrate the σ phase. Note that in order to be consistent with the mobilities used in the literature the constitutive equation, equation (3), does not use charge times mobility. The effect of charge is included in the mobility. Diffusive and dispersive mechanisms will definitely affect broadening of peaks over long time periods, but since they do not affect the species velocity, we neglect them in this analysis. Combining equations (2) and (3) we obtain

$$\varepsilon \frac{\partial c_i}{\partial t} + \nabla \cdot \varepsilon (c_i v - c_i u_{i\beta} F \nabla \Psi) = - m \tag{4}$$

where for simplicity all the subscripts and brackets in the interstial concentration and velocity have been dropped. The quantity *m* is the molar transport rate represented by the last intergral on the right hand side of equation (2).

A similar equation can be derived for the average concentration of species i in the solid phase. The flux equation is of similar form to equation (3) as shown in Appendix A. The average concentration in the solid phase consists of the protein in the pores of the solid, n_i, and the protein bound to the solid, N_i. Both n_i and N_i are given in moles of protein per unit volume of particle. In the solid there is no convection, and the ionic mobility can be different from that in the fluid. The volume fraction of the solid phase is $(1-\varepsilon)$ so that the volume averaged form of the continuity equation for species i becomes

$$(1-\varepsilon)\frac{\partial n_i}{\partial t} + (1-\varepsilon)\frac{\partial N_i}{\partial t} - \nabla \cdot (1-\varepsilon)\, u_{i\sigma} n_i F \nabla \Psi = m \qquad (5)$$

where $u_{i\sigma}$is an effective mobility in the gel. Note that only the protein in the pores, but not that bound to the particle, has significant electrophoretic motion. The potential gradient is taken to be uniform inside and outside the particles, reflecting the ease of transport of small ions through the entire column volume.

If we sum equations (4) and (5), we obtain an equation for the total concentration of a given solute in the bed

$$\frac{\partial}{\partial t}[\varepsilon c_i + (1-\varepsilon)(n_i + N_i)] + \nabla \cdot \{\varepsilon c_i v - F[\varepsilon u_{i\beta} c_i + (1-\varepsilon) u_{i\sigma} n_i] \nabla \Psi\} = 0 \qquad (6)$$

The potential Ψ, the species concentrations n_i and c_i, and the interstitial velocity are taken to be uniform over the column cross-section. If the flow is one dimensional the equation above can be written in terms of the variation with axial position x and time t

$$\frac{\partial}{\partial t}[\varepsilon c_i + (1-\varepsilon)(n_i + N_i)] + \frac{\partial}{\partial x}\{\varepsilon c_i v - F[\varepsilon u_{i\beta} c_i + (1-\varepsilon) u_{i\sigma} n_i] \frac{\partial \Psi}{\partial x}\} = 0 \qquad (7)$$

The potential Ψ may be found by using the requirement that the fluid and the particles must be electrically neutral at each point[11], namely, that

$$\sum_{i=1}^{M} z_i c_i = 0, \qquad (8)$$

and

$$\sum_{i=1}^{M} z_i (n_i + N_i) + \sigma = 0$$

where σ is the surface charge on the packing. Multiplying equation (7) by z_i, summing over all species M, and using equations (8) and (9) gives

$$\frac{\partial}{\partial x} \left\{ \sum_{i=1}^{M} z_i F [\varepsilon u_{i\beta} c_i + (1-\varepsilon) u_{i\sigma} n_i] \frac{\partial \Psi}{\partial x} \right\} = 0 \qquad (9)$$

The term inside the derivative can only be a function of time. In fact, this is the negative of the current I(t), so that

$$\sum_{i=1}^{M} z_i F [\varepsilon u_{i\beta} c_i + (1-\varepsilon) u_{i\sigma} n_i] \frac{\partial \Psi}{\partial x} = - I(t) \qquad (10)$$

This is the governing equation for the potential gradient, and the term

$$\Omega = \sum_{i=1}^{M} z_i F [\varepsilon u_{i\beta} c_i + (1-\varepsilon) u_{i\sigma} n_i] \qquad (11)$$

represents the overall electrical conductivity of the column.

In general, electrophoresis processes can be operated by fixing either the current or the voltage drop across the column. The value of I(t) will be given as a boundary condition for the cases where the current is either a constant or controlled to be a known function of time. The constant potential problem will require specification of the potential at both boundaries of the column.

Further simplification is possible for the protein separation problem where the current carrying buffer can have molar concentrations three orders of magnitude or more larger than the protein concentration. In this case the conductivity in equation (11) is dominated by the buffer species terms, and it is thus relatively constant throughout the column. In this case Ω can be treated as being constant, and the equation for the potential Ψ can be integrated to yield

$$\frac{\Psi_L(t) - \Psi_o(t)}{L} = - I(t) / \Omega \qquad (12)$$

This gives the relation between voltage drop and current for a system of constant conductivity. Thus, if the conductivity is assumed constant, equation (12) can be used to determine the current for a given potential drop, or to determine the potential for a given applied current. For a given buffer concentration and mobility it is possible that as the protein concentration increases there will be a time when the protein will affect the electrical field. For example, consider a tris acetate buffer with a concentration of 10 mM and with mobilities of -27.8 x 10^{-5} and 44.6 x 10^{-5} cm^2/V-sec for tris and acetate, respectively[12]. In this case for ferritin at pH 7.4, with a mobility of 10^{-4} cm^2/V-sec and a charge of 10, a concentration of 5 x 10^{-4} molar will have a 10% contribution to the sum in equation (11). Starting concentrations of 10^{-5} to 10^{-7} molar would thus allow concentration increases of 50 to 5000 times before significant field effects arise. For proteins with lower mobilities, i.e. 10^{-5} cm^2/V-sec and a charge of 1, the concentration would have to approach 5 x 10^{-2} molar to have a 10% contribution to the sum in equation (11). The experimental section of this paper describes the results of measurements of the conductivity of both agarose and polyacrylamide gel particles with and without protein. The results of these experiments validate the assumptions made in equation (12).

In order to relate c_i, n_i, and N_i it is necessary to make some assumptions about the mass transfer characteristics of the process. The Stanton number, kL/v, is the ratio of mass transfer resistance to convective flow, where k is the mass transfer coefficient, L is the bed length, and v is the interstitial velocity. The mass transfer resistance consists of the external phase mass transfer resistance for the transfer from the bulk fluid to the particle surface, and the internal mass transfer resistance for the transfer within the particle. Estimates of the external and internal mass transfer coefficients from standard correlations[13] give values of 4 to 8 min^{-1} and 1 to 3 min^{-1}, respectively. Adding the mass resistances requires adding the reciprocal of the mass transfer coefficients. For a 10 cm long column and a velocity of .3 cm/min the Stanton numbers are of order 20 to 80. This indicates that mass transfer resistance may be of importance. However, mass transfer resistance effects do not affect the criterion for accumulation, although they will affect the concentration profiles in the column at any particular time. Thus, for our initial analysis we shall neglect mass tranfer resistance.

As a result of neglecting mass transfer resistance an equilibrium is established between the species i in the bulk fluid and in the pores of the solid particles. It is assumed that the concentration of the fluid in the pores of the gel would be equal to that in the bulk solution. Therefore, n_i, the concentration in the pores per unit volume of particles can be written in the form

$$n_i = \beta_i' c_i \tag{13}$$

where β_i' is the average porosity of the particles in the bed for species i. It is given in units of volume of pores to volume of bed.

In addition, it can be assumed that the distribution between the protein in the fluid pores of the particles and the protein bound reversibly to the particle also has a linear distribution of the form

$$N_i' = c_i K_i' \tag{14}$$

where K_i' is the adsorption equilibrium constant and N_i' is the moles of protein bound per volume of fluid. Thus, N_i, the moles of protein bound per volume of particles, is given by

$$N_i = N_i' \beta_i' = \beta_i' K_i' c_i \tag{15}$$

Certainly at very high concentration this relationship will no longer be linear, however for our initial analysis we will assume that it is linear. Note also that K_i' is a dimensionless constant that relates the moles bound per volume of fluid to moles in the fluid per volume of fluid.

In equation (13) the units of n_i are moles per volume of total particles and those of c_i are moles per volume of fluid. The parameter β_i' thus has the units of volume of fluid accessible to species i divided by the total volume of particles. The amount of accessible fluid varies down the length of the column due to the variation in packing types and to the variation in the relative proportions of packing types. The internal porosities, β_{io} and β_{il}, of the polyacrylamide and agarose gel particles, respectively are intensive properties of the specific packings, i.e. they do not vary with the amount of the packing. In order to account for the axial variation of the internal porosity it is necessary to consider the change in the relative volumetric proportions of the two packings. The volume of polyacrylamide

particles to total particle volume is given by λ_o, and the volume of agarose particles to total particle volume is given by λ_1. Note that $\lambda_o + \lambda_1 = 1$. We now can consider β_i' as the sum of two parts

$$\beta_i'(x) = \beta_{io}\lambda_o(x) + \beta_{i1}\lambda_1(x) \tag{16}$$

It should be noted that equation (16) may not be valid when the proportion of either particle becomes so small that the small number of particles present do not give a uniform distribution across the cross-section of the column.

Similarly, the adsorption constants κ_{io} and κ_{i1} for the polyacrylamide and agarose particles respectively are intensive properties of the packing types. Thus we also allow K_i' to consist of the sum

$$K_i'(x) = \kappa_{io}\lambda_o(x) + \kappa_{i1}\lambda_1(x) \tag{17}$$

Using equation (10) for the potential gradient, equation (11) for Ω, equation (13) for n_i and equation (15) for N_i, it is possible to write equation (7) in the form

$$\frac{\partial c_i}{\partial t} + \frac{1}{1 + \frac{1-\varepsilon}{\varepsilon}\beta_i'(x)(1+K_i'(x))} \cdot \tag{18}$$

$$\frac{\partial}{\partial x}\left\{ c_i v + \frac{c_i u_{i\beta} IF\,[1+(1-\varepsilon)\beta_i'(x)\Phi_i'(x)/\varepsilon]}{\Omega} \right\} = 0$$

where

$$\Phi_i' = \phi_{io}\lambda_o(x) + \phi_{i1}\lambda_1(x) \tag{19}$$

Here the quantities ϕ_{io} and ϕ_{i1} are equal to $u_{i\sigma}/u_{i\beta}$ the ratio of the electrophoretic mobilities of the species in the pores of the solid to that in the bulk fluid, in the polyacrylamide and agarose particles respectively. The ϕ's are also

intensive properties of the packings. It is commonly assumed in the electrophoresis literature[14] that $\phi = \beta$. This will be also assumed in our analysis. However, it should be noted that alternative expressions[14,15] are sometimes used to relate ϕ to β. The external void fraction ϵ is taken to be a constant independent of position. This implies that the interstitial velocity v will also be constant. Since most electrophoretic processes can be carried out at constant current or constant potential, I in equation (13) is treated as being time-independent.

The following dimensionless variables can be defined

$$\begin{aligned}
&\tau = tv/L \\
&s = x/L \\
&C(s,\tau) = c/c_o \\
&\alpha(s) = (1-\epsilon)\beta'(x)/\epsilon \\
&\mu = (u_\beta IF/\Omega)/v \\
&\Phi(s) = \Phi'(x) \\
&K(s) = K'(x)
\end{aligned} \tag{20}$$

so that equation (19) can be written in the form

$$\frac{\partial C}{\partial \tau} + \frac{1}{1 + \alpha(s)(1+K(s))} \frac{\partial}{\partial s} \left\{ C[1+\mu(1+\alpha(s)\Phi(s))] \right\} = 0 \tag{21}$$

Note, the species subscript i has been dropped. From now on this equation is applied only to the protein of interest. In equation (20) L is the total column length, and the parameter $\alpha(s)$ represents the total volume of accessible fluid within the pores per volume of fluid outside the pores. This parameter is always greater than zero. The parameter μ is a measure of the ratio of electrodiffusive to convective transport. Since it depends on u_β, each species has a given value of μ with which it can be associated. In fact μ can be either positive or negative depending on the signs of the mobility and the current I.

Equation (21) is similar to that used by McCoy[7], however in his analysis he has neglected the mobility ratio term Φ.

Solution by the Method of Characteristics

Equation (21) is a linear first order hyperbolic partial differential equation which can be solved by the method of characteristics[16]. It can be expanded to give

$$\frac{\partial C}{\partial \tau} + \frac{1}{1+\alpha(s)(1+K(s))}[1+\mu(1+\alpha(s)\Phi(s))]\frac{\partial C}{\partial s} \tag{22}$$

$$+ \frac{C\mu}{1+\alpha(s)(1+K(s))}\frac{d(\alpha(s)\Phi(s))}{ds} = 0$$

The characteristic equations, in terms of a parameter, ω, which varies along the characteristic curves, are written as

$$\frac{d\tau}{d\omega} = 1$$

$$\frac{ds}{d\omega} = \frac{1+\mu(1+\alpha(s)\Phi(s))}{1+\alpha(s)(1+K(s))}$$

$$\frac{dC}{d\omega} = -\frac{C\mu}{1+\alpha(s)(1+K(s))}\frac{d(\alpha(s)\Phi(s))}{ds} \tag{23}$$

When $\alpha(s)$, $K(s)$ and $\Phi(s)$ are constant, the concentration is constant along a characteristic and when $\alpha(s)$, $K(s)$ and $\Phi(s)$ are not constant the concentration will increase or decrease along a characteristic depending upon the sign of μ and the sign of the derivative $d(\alpha(s)\Phi(s))/ds$.

The motion of the species of interest is reflected by the slope of the characteristic curves emanating from the boundaries at $s=0$ and $s=1$, and from the initial conditions at $\tau=0$. The slope of the characteristic curves is given by

$$\frac{d\tau}{ds} = \frac{1+\alpha(s)(1+K(s))}{1+\mu(1+\alpha(s)\Phi(s))} \tag{24}$$

Since the hyperbolic equation is linear the characteristic curves are fixed for a given set of parameters. The solution of equation (24) gives the relationship between τ and s for any boundary or initial conditions.

The nature of the functional forms for $\alpha(s)$, $K(s)$ and $\Phi(s)$ depends upon the way the column has been packed, and thus upon the nature of the function $\lambda_o(x)$. If there is a very sharp transition between the acrylamide gel particles and the agarose gel particles the functional forms for $\lambda_o(x)$, $\alpha(x)$, $K(x)$ and $\Phi(x)$ would approach step changes. Physically, there is always some finite region over which the properties change from one type of packing to the next. For the purposes of illustration it is assumed that $\lambda_o(x)$ is a linear function of s (or x) in a region between $s=s_o$ and $s=s_1$. It takes on a constant value for the acrylamide gel in the region $s<s_o$ and it has a constant value for the agarose gel when $s>s_1$. This assumption implies a linear variation for $\alpha(s)$, $K(s)$, and $\Phi(s)$.

Figure 2 illustrates the characteristic curves in the τ-s plane for various values of μ. For μ less than $-1/(1+\alpha_o\Phi_o)$ all the characteristics have negative slope. This implies that the state of the bed is influenced only by the initial condition at $\tau=0$ and the boundary condition at s=1. The boundary at s=0 does not influence the column. Physically, this means that the applied potential is so high that the protein in the feed cannot propagate into the bed. Ultimately the bed will empty as all the proteins migrate out the top and no protein enters at the bottom.

When μ is greater than $-1/(1+\alpha_1\Phi_1)$ all the characteristics have positive slope. In this case the state of the bed is influenced only by the initial state and the boundary state at s=0. This implies that the applied potential is so low that all the protein will wash out the end with the convective flow.

For μ in the region between the two limiting values, i.e.

$$-\frac{1}{1+\alpha_o\Phi_o} < \mu < -\frac{1}{1+\alpha_1\Phi_1} \tag{25}$$

the characteristics from the top of the bed have positive slope and the characteristics from the bottom of the bed have negative slope. In this case the protein is moving toward some point within the column from both sides of the region where the two different particle packing types meet. This will give accumulation within the column. Since the slopes of the characteristics change from positive on the upstream side to negative on the downstream side they must be infinitely large at some point between s_o and s_1. Since Φ and α are always positive it is clear from equation (13) that $\mu < 0$. This means that the electrophoretic motion must always

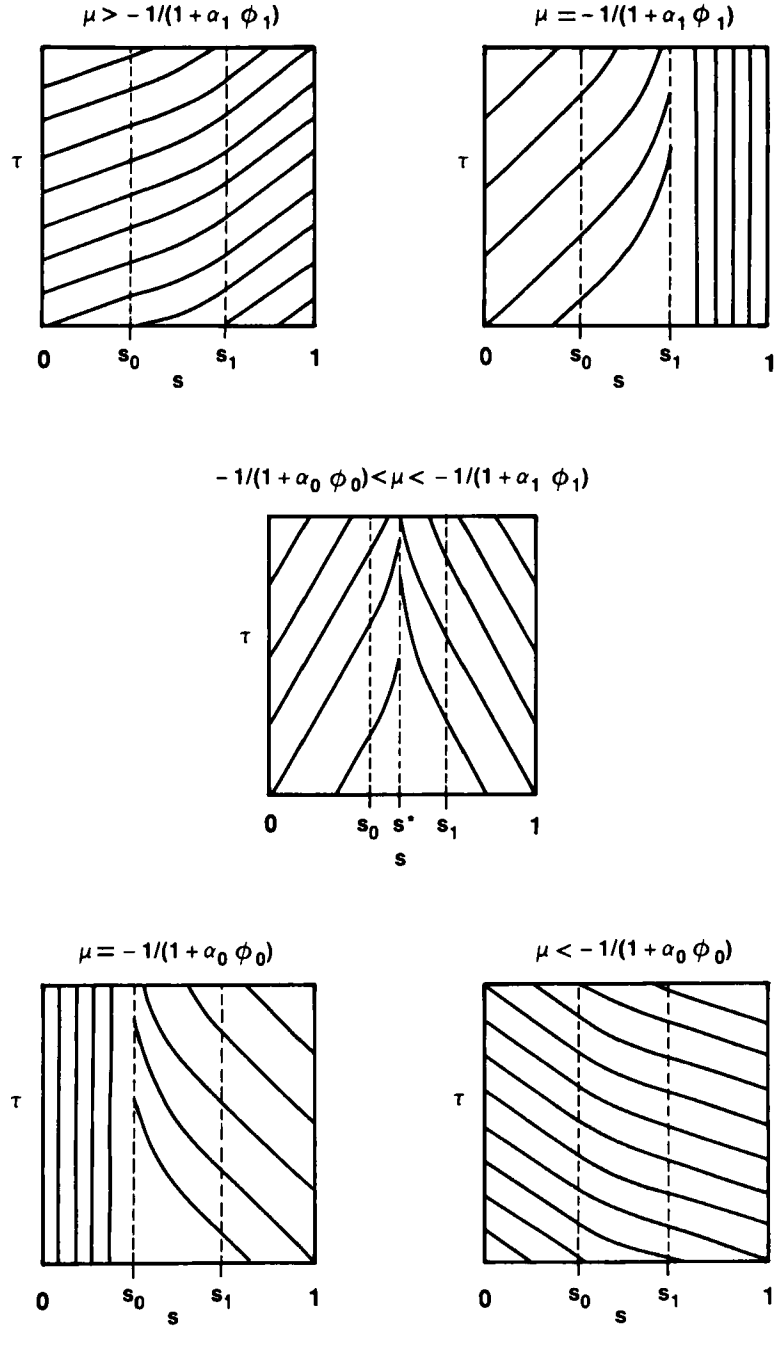

FIGURE 2
Variation of the Characteristic Plane with μ

be oriented in the opposite direction from the flow. The electric field direction desired will depend on the sign of the mobility. Equation (25) can be written as

$$\frac{1}{1+\alpha_o\Phi_o} > |\mu| > \frac{1}{1+\alpha_1\Phi_1} \tag{26}$$

Furthermore, since α and Φ are always positive, equation (26) implies

$$|\mu| < 1 \tag{27}$$

This implies that the magnitude of the motion due to the electrical migration must always be less than that due to the convective flow. Equation 26 indicates that in order to narrow the range of $|\mu|$ that will lead to accumulation one needs to make the β's for the two packings closer in magnitude. This narrowing of the accumulation region for one protein will cause other proteins to pass through the column, and thus facilitate the separation of a single species.

It is important to note that the presence of adsorption does not affect the criterion for accumulation since it does not affect the term in the denominator of equation (24). Adsorption will not determine whether accumulation will occur or not, however, it will have a significant affect on the magnitude of the resulting concentration. Adsorption can only affect the accumulation if the protein moves by electrophoresis from adsorbed site to adsorbed site without going back into the solution phase. Only in this case will the adsorption effect appear in the last term of the left hand side of equation (5), and thus eventually appear in the accumulation criterion. As mentioned previously, in this analysis it is assumed that bound protein does not move by electrophoresis.

The experimental methods and results for the work in our study will be presented in the next section. The accumulation criterion, equation (26) will be tested with this data.

EXPERIMENTAL METHODS

Apparatus

Figure 3 shows a schematic of the experimental apparatus used in the present study. A 1.1 cm internal diameter glass column 9.5 cm long was constructed with

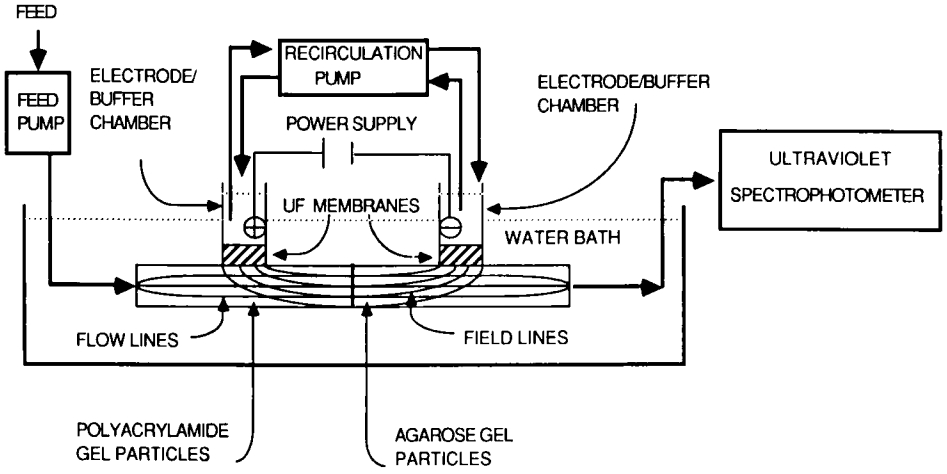

FIGURE 3
Experimental Apparatus

one number 11 Ace Glass threaded fitting at each end. This allowed 9.5 cm of total packing to be placed in the column. Generally, half of the column was packed with polyacrylamide and half was packed with agarose gel filtration particles. P-10 polyacrylamide and A-5 and A-150 agarose gel filtration particles from BioRad were used. Table I summarizes the properties of the gels used in this study. Two Ace Glass threaded fittings were attached at right angles to the main axis of the glass column. These fittings were spaced 6 cm apart on the same side of the column. Two 300 ml glass reservoirs were connected to these two right angle fittings via Teflon (R) threaded fittings and FETFE (R) o-rings. These reservoirs served as chambers for the platinum wire electrodes.

Each electrode consisted of a 25 cm long 28 gauge platinum wire with a 2.5 cm by 2.5 cm 52 mesh platinum gauze attached to the ends of the wire. All platinum was obtained from Fisher Scientific. An LKB model 2301 Macrodrive power supply was used to provide the electrical current and field.

Spectro/Por (R) (Spectrum Medical Industries, Inc.) molecular porous ultrafiltration membranes (UF) with molecular weight cutoffs of approximately

TABLE I

Gel Properties

Packing	Diameter (μ)	Range (Daltons)	ε
Polyacrylamide (P-10)	150-300	$1.5x^3$-$2x10^4$	0.37
Agarose (A-5)	150-300	10^5-$5x10^7$	0.37
Agarose (A-150)	150-300	10^6-$1.5x10^8$	0.37

3500 Daltons were used to separate the electrode reservoirs from the column. A fluorocarbon screen mesh, also from Spectrum Medical Industries, Inc., was used with the UF membrane to provide mechanical support. The UF membrane and the fluorocarbon screen were cut to fit between the Teflon (R) threaded fittings and the glass threaded fittings. The o-rings provided a tight seal.

Approximately 200 ml of buffer solution was placed in each of the electrode reservoirs. This solution was recirculated between the two chambers to prevent any pH gradients from forming due to the reactions at the electrodes. The input to each chamber from the recirculation pump was allowed to fall dropwise into the reservoirs so as to prevent electrical contact between the chambers.

The entire column with the two electrode reservoirs was placed horizontally in a room temperature water bath as shown in Figure 3. The feed solutions were pumped in as shown, and the output was monitored with a Bausch and Lomb Spectronic 21 ultraviolet spectrometer at various wavelengths between 210 nm and 340 nm. The colored proteins horse spleen ferritin, horse skeletal muscle myoglobin, and horse heart cytochrome-c were all obtained from Sigma Chemical Company. Table II summarizes some of the molecular properties of these three proteins. The buffer solutions used for both the protein feed and the electrode chambers were 10 mM tris acetate (Sigma Chemical Company). The pH was adjusted with 1 N NaOH and 1 N HCl.

Procedure

The external porosity of the bed can be easily measured by the breakthrough response of the bed, with no applied electrical field, for large molecular weight

TABLE II.
PHYSICAL PROPERTIES OF PROTEINS

Protein	Molecular weight[18]	Diffusion Coefficient[17] cm^2/sec	Isoelectric Point	Molecular Radius nm	Mobility x F $cm^2/V\text{-}sec$
Ferritin	450,000	3.5×10^{-7}	4.5	5.09	-5 to -17 x1 0^{-5} at pH 6.8 - 8.8[19]
Myoglobin	17,800	11.3×10^{-7}	6.9	1.73	6×10^{-5} at pH 5.1[20]
					$> -5 \times 10^{-5}$* at pH 9.3[20]
Cytochrome -C	12,400	11.4×10^{-7}	10.5	1.53	7×10^{-5} at pH 7.4[21]

* - literature value was not determined at pH above pH 8.4

proteins or other molecules that do not penetrate the pores of the packing or adsorb to the packing. BioRad[22] product literature states that the average external porosity for all their agarose and polyacrylamide gel filtration packing is .33. Breakthrough analysis of ferritin, a large molecular weight protein that is completely excluded from the polyacrylamide gel particles P-10, gave ε=.37 for these P-10 particles. It was thereafter assumed for all subsequent Biorad gels that ε was equal to this value.

Breakthrough responses for all the proteins in the agarose gels were also measured. The results for these measurements will be discussed in the next section.

The accumulation experiments were run as follows. The protein solutions of concentrations 10^{-5} to 10^{-7} molar were loaded into the column with the electrical field off. Thereafter, the feed was switched to pure buffer and the electrical field was turned on. The potential was varied until protein was accumulated at the interface between the two packings. Since all the proteins used in this study were colored, this accumulation could easily be monitored by eye. Once a band had formed, the potential was increased until the protein just started to migrate in the upstream direction. This determined the upper limit of the potential for accumulation. The potential was then lowered until the protein just started to move downstream with the convective flow. This was considered to be the lower limit of the potential. Since the flow rates were fairly low, of order .1 to .3 ml/min, it was easier to vary the electrical field than to vary the flow rates in order to determine the upper and lower accumulation potentials.

Experimental Results

Table III summarizes the results of accumulation experiments for ferritin at pH 7.4, myoglobin at pH 9.3 and 5.1, and cytochrome c at pH 7.4. The upper limit in the accumulation criterion, equation (26), was taken as 1.0 for the ferritin and myoglobin because neither protein adsorbed or penetrated the pores of the polyacrylamide gel particles, P-10, i.e. β=0. The upper limit for the cytochrome c was 0.98 since it had some penetration into the P-10 gel. Using the accumulation criterion, equation (26), and the measured potential for which accumulation occurred, the mobility was calculated.

The largest measured potential that would allow accumulation was used in this calculation. Table III lists the mobilities calculated in this manner for the three proteins. The mobilities for ferritin, cytochrome, and myoglobin were fairly close to the literature values (shown in Table II) for the same pH value.

TABLE III.
PROTEIN ACCUMULATION DATA

Protein (pH) (Gel pair)	Upper Bound	Lower Bound	Mobility x F cm^2/V sec	K	$\beta = \Phi$ (fit)	$\alpha(1 + K)$ (Breakthrough results)
Ferritin (pH 7.4) (P10/A5)	1.0	0.66	-8.3×10^{-5}	0	.55	1.7
Myoglobin (pH 5.1) (P10/A5)	1.0	0.63	9.7×10^{-5}	12.9	.60	23.7
Myoglobin (pH 9.3) (P10/A5)	1.0	0.67	-6.3×10^{-5}	0.85	.54	3.2
Cytochrome-C (pH 7.4) (P10/A150)	0.98	.83	8.8×10^{-5}	12.1	.35	22.3

TABLE IV

Experimental Conditions used by O'Farrell[1] for Protein Accumulation

Column:	50 cm long, 0.7 cm diameter
Flow rate:	0.17 ml/min (Ferritin)
Voltage drop:	12 V/cm (Ferritin)
Buffer:	10 mM Tris Acetate pH 7.4
Buffer-Column Barrier:	Polyacrylamide Plug
Packing:	P-10/A-5 (Ferritin)

Using the measured lower potential for accumulation the lower bound in the accumulation criterion, equation (26), could be calculated. These lower bounds could then be used to calculate β. It was also assumed that $\beta = \phi$, i.e. that the ratio of the protein mobility in the particle to that in the free solution was equal to the pore volume fraction. This is a commonly used assumption in gel electrophoresis[14,15]. Once β was determined in this fashion κ could be calculated using the results of breakthrough curves where no field was applied.

The κ value of 0 for ferritin reflects no adsorption at this pH. However, other experiments with ferritin at a pH of 3 gave extensive irreversible adsorption to the agarose gel. No value of κ was determined for this case of irreversible adsorption to the agarose gel. Since the isoelectric point of ferritin is 4.5 it will have a positive charge at pH 3, and will thus interact with the negatively charged agarose. Myoglobin, with an isoelectric point of 6.9, gave strong reversible adsorption to the agarose at the lower pH. The adsorption effects were not totally eliminated at the higher pH of 9.0. Cytochrome-c, with an isoelectric point of 11, also showed strong reversible adsorption at pH 7.4.

The accumulation data of O'Farrell[1] did not fit the accumulation criterion proposed in our model. However, we were not able to repeat O'Farrell's original experiments. For the same interstitial velocity, the same packing, the same pH and buffer and the same applied field per unit length as in O'Farrell's published results we were not able to get the proteins to accumulate in the column. Table IV lists the conditions for which O'Farrell was able to get ferritin to accumulate. We were able to get accumulation for the conditions reported in Table V.

TABLE V

Experimental Conditions used in Present Study

Column:	10 cm long, 1.1 cm diameter
Buffer:	10 mM Tris Acetate, varying pH

Protein	Flow (ml/min)	Voltage Drop (V/cm)	Gel	pH
Ferritin	0.15	54-85	P-10/A-5	7.4
Myoglobin	0.27	83-133	P-10/A-5	5.1
Myoglobin	0.06	50-75	P-10/A-5	9.3
Cytochrome-C	0.18	80-95	P-10/A-150	7.4

Thus, in conclusion our accumulation criterion appeared to be reasonable. The mobilities calculated from the criterion for our experimental accumulation conditions agreed with literature values of protein mobilities for ferritin and myoglobin. In addition, adsorption constants and internal porosities calculated from the criterion and breakthrough results appeared to be of reasonable magnitudes.

Equipment Design

The basic principle of CACE requires that the electrical field be parallel to the convective flow field at the interface between the two packings. Furthermore, it is necessary that both fields are uniform across the column cross-section at this interface. However, since it is also necessary to isolate the electrodes from the flowing fluid, the electrical field at the column entrance and exit cannot be parallel to the flow field. This is illustrated in Figure 3 where the flow lines and field lines are shown schematically. If there are such regions at the ends of the column where the fields are not parallel it is possible that proteins will collect at the column ends in addition to, or rather than, at the interface between the two packings.

The importance of these end effects can be readily observed by continuously feeding the protein solution into the column while the electrical field is on. When the field polarity is oriented so that the protein, for example ferritin, should

accumulate, and indeed does accumulate at the interface between the two packings, it is observed that some ferritin also accumulates near the upper electrode.

In addition to the end effects, other considerations in the design of the column include the choice of the gels, their hydrodynamic properties as well as sieving properties, the effects of mass transfer resistance, the presence of electroosmosis, wall effects, heat generation, and the protein concentration effects at the interface.

The gel filtration media used in the present study generally imposes significant constraints on the operating flow rates due to large pressure drops and compressibility. The typical operating linear velocities for these gels range from 2 to 10 cm/hr. For our column with a cross-sectional area of 0.95 cm^2 this corresponds to flow rates of 0.03 to 0.16 cc/min. It appears that in order to increase the size and throughput for the CACE process it is necessary to find packing with better flow characteristics. However, it is also necessary to insure that this packing does not significantly alter the electrical field properties in the column; i.e. the basis of the separation requires that the electrical field through the particles be the same as in the pore space of the column.

The conductivities of the agarose and polyacrylamide gels were evaluated using the same apparatus used for the accumulation runs. However, in this case the column was packed with only one gel at a time. The voltage was set at values from 0 to 1000 volts and the current was measured for each voltage. The solutions used were 10 mM tris acetate adjusted with 3.6 ml of 1N NaOH per liter of buffer to pH 7.4. Figure 4a shows the current versus voltage data for the polyacrylamide gel packing (P-10). This figure shows some vairability from run to run for a given flow rate in the column. In addition, in one run ferritin at a concentration of 10^{-5} M was pumped together with the buffer into the column. It accumulated near the electrode, however little effect on the resulting current was observed. This figure also shows little effect of a reversed field polarity on the resulting current. Figure 4b shows the current versus voltage data for the agarose gel particles (A-5). Again added protein (10^{-5} molar ferritin or 10^{-5} molar myoglobin) had little effect on the current. Figure 4c combines the data for the agarose and polyacrylamide gel particles. The error bars show the range of currents given in the previous two figures. Although there is some variability in the currents there is also significant overlap for the two packings. Thus, the conductivities of the two sections of the column can be assumed equal for the purposes of our initial analysis, and it can be taken to be independent of protein concentration for the range of concentration used in our experiments. This observation supports the assumptions made in deriving

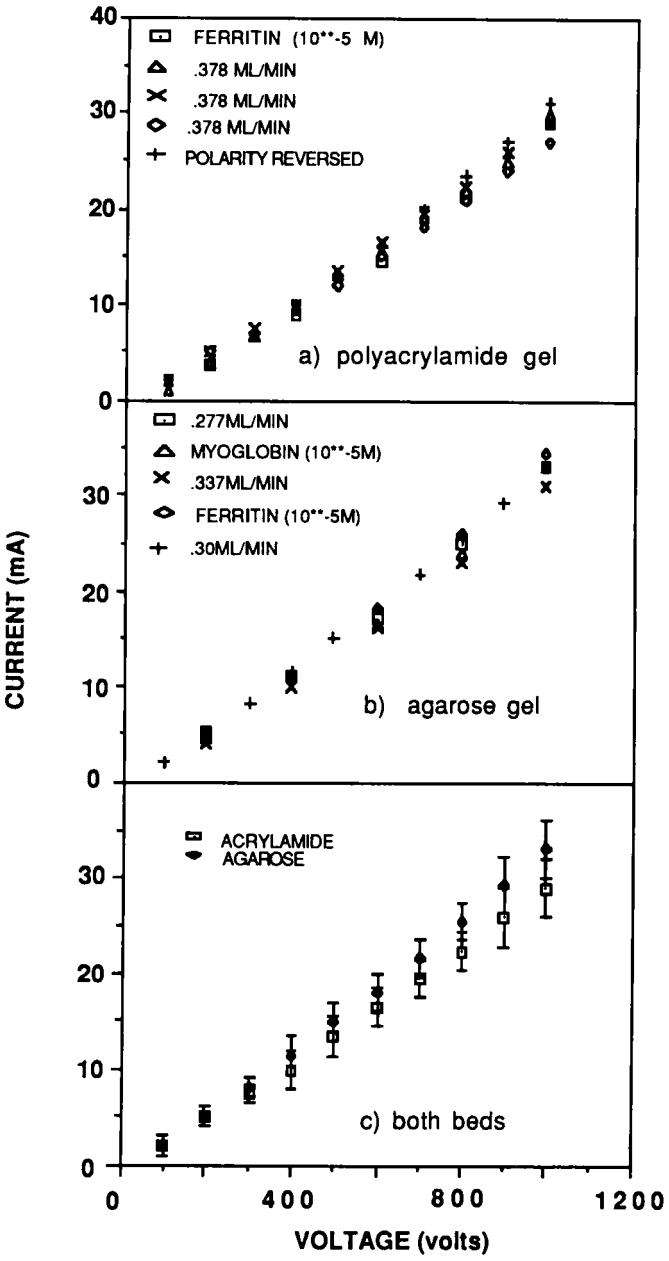

FIGURE 4
Bed conductivities

equation (12), namely, that the buffer ions are primarily responsible for carrying the current in the system, that the proteins do not affect the conductivity, and that both sections of the column have equal conductivities.

Electroosmosis, also termed electroendoosmosis, refers to the flow induced by counterion motion when a charged surface is placed in an electric field. Electroosmosis has been a concern in the past with agarose gels, however recent formulations have reduced the charge on the agarose surfaces. Indeed, measurements of the A-150 agarose particles on a zeta potential meter indicated no measurable surface charge. Additional evidence against electroosmosis is that the flow and pressure drop in the column were not observed to change with the application of the electric field.

Several breakthrough runs were made with urea, a small relatively uncharged molecule that should penetrate the entire column volume and that can be readily observed with the UV spectrophotometer at 210 nm. With urea the same breakthrough was observed with the field off as with the field on with either polarity orientation. This indicated that electroosmotic flow does not cause holdup in the column.

Fixed charges on the walls of the glass column can also lead to electroosmosis. Herrin et al[23] studied electroosmotic flow in glass capillaries. However, since the column diameter is of order 1 cm the influence of any charge on the glass walls would not extend into the column, and would thus have negligible effect on the flow. Some data for ferritin accumulation suggest that wall effects at the interface may occur; i.e. the ferritin appeared to begin accumulating near the walls of the column, however, this effect seemed to occur only at the early times where small amounts of ferritin had accumulated.

Heat generation can be estimated by the relationship q=IV where q is the rate of heat generation, I is the current, and V is the voltage. Using this equation and measurements of current and resistance indicate that at operating conditions of 800 volts and currents of 5mA gave a heat generation of 1 cal/sec. It is generally necessary to use a water bath to keep the system cool; however care should be taken in lowering the temperature because the flow resistance increases at lower temperatures due to higher viscosities. It is also more convenient to run the system in a horizontal position so as to easily cool the entire apparatus.

The rate of mass transfer from the bulk fluid to the internal pores of the packing may have a significant effect on the system design. Mass transfer resistance will

not affect the accumulation criterion. However, it will affect the concentration profile within the column. Large mass transfer resistance will cause the concentration in the lower portion of the column to spread. This would make it necessary to use longer columns or to recirculate the fluid leaving the column so as to prevent excess loss of desired protein.

As protein accumulates within the column it may be possible that it will begin to have an effect on the potential field. This was not observed to occur in our experiments where the current did not appear to vary significantly as the protein concentrated in bands in the column. It is also possible that the upper limit in protein concentration may be reached due to protein solubility limits. Indeed this may occur before any significant effects on electrical field take place. Concentration increases of roughly 20 times were observed in our experiments. This estimate was based on the relative size of the accumulated protein region to the length of the column. It is desirable to run CACE system at pH values where the protein of interest have their highest net charge; i.e far from their isoelectric points where they have higher solubility. It is also necessary to run at pH's so that the charges do not cause irreversible binding to the packing as was observed for ferritin in the agarose at pH 3.0.

TRANSIENT CALCULATIONS

The foregoing work has emphasized the determination of the conditions that will cause a protein to accumulate in the column. It is also of interest to determine the rate of increase of the concentration of the accumulated protein at the interface and its final steady-state concentration for a continuous process. Hunter[9] has developed a steady-state model that attempts to determine the accumulated protein concentration. She assumes that all of the protein is in some region at the interface and that this protein affects the electrical field. Using the accumulation data of O'Farrell[1] she finds concentrations of about an order of magnitude less than those experimentally found by O'Farrell. However, since we were unable to repeat O'Farrell's experiments this comparison of her model with his results may not give an adequate test of her model.

Our approach to determining the concentration at the interface is to utilize the simple first order hyperbolic equations, neglecting mass transfer and axial dispersion, developed previously. Since the equations are hyperbolic it is necessary to define an averaging region over which to write another mass balance. In the following section the theoretical model will be solved to illustrate the transient

aspects of the system. Numerical results will be given to show the behavior for several cases with simplified parameters.

Figure 5 illustrates that τ-s characteristic plane and the functional form for $\lambda(s)$ for the case of $|\mu|$ within the limits imposed by equation (26). It is assumed for the purposes of illustration that λ_0 is a linear function of s in a region between $s = s_0$ and $s = s_1$. This implies that $\alpha(s)$, $K(s)$ and $\Phi(s)$ are also linear functions of s in this region. The size of the region $s_1 - s_0$ depends upon how the particles are packed in the column. If the two packing materials are not mixed, the boundary between the two may be fairly sharp, and thus $s_1 - s_0$ would be of order of several particle diameters divided by the bed length. However, it is possible to pack the column so that $\lambda(s)$, $K(s)$, $\alpha(s)$ and $\Phi(s)$ vary linearly throughout the length of the column by mixing the bed materials so that the proportion of each particle type varies linearly. In this case $s_1 - s_0 = 1$. We will primarliy be concerned with $s_1 - s_0$ small. We shall develop the general equations for any $s_1 - s_0$. It can be noted that the larger $s_1 - s_0$ the greater the resolution for more than one protein. We shall illustrate the single component concentration increase for the case of small $s_1 - s_0$, and we shall illustrate the multicomponent case for large $s_1 - s_0$.

In Figue 5 on the upstream side of the region of variable $\lambda(s)$, $\alpha(s)$ is a constant equal to α_0, i.e. $\beta' = \beta_0'$, $K(s) = \kappa_0$ and $\Phi(s) = \phi_0$. On the downstream side $\alpha(s) = \alpha_1$, i.e. $\beta' = \beta_1'$, $K(s) = \kappa_1$ and $\Phi(s) = \phi_1$. In the region where α, K and Φ are constant the slopes of the characteristics are straight lines, and concentrations along the characteristics are constant. Once the characteristics enter the region between s_0 and s_1 the slopes are no longer constant, and the concentration will vary along the characteristics.

The solute will accumulate in the region between s_0 and s_1. As the solute accumulates, the centroid of the concentration profile will be near s*. The value of s* corresponds to the position in the column where the slope of the characteristics, given by equation 24, becomes infinite. This is given by

$$\alpha(s^*)\,\Phi(s^*) = \frac{1 - |\mu|}{|\mu|} \tag{28}$$

After accumulation starts, some band spreading will occur due to hydrodyanmic dispersion and diffusion effects.

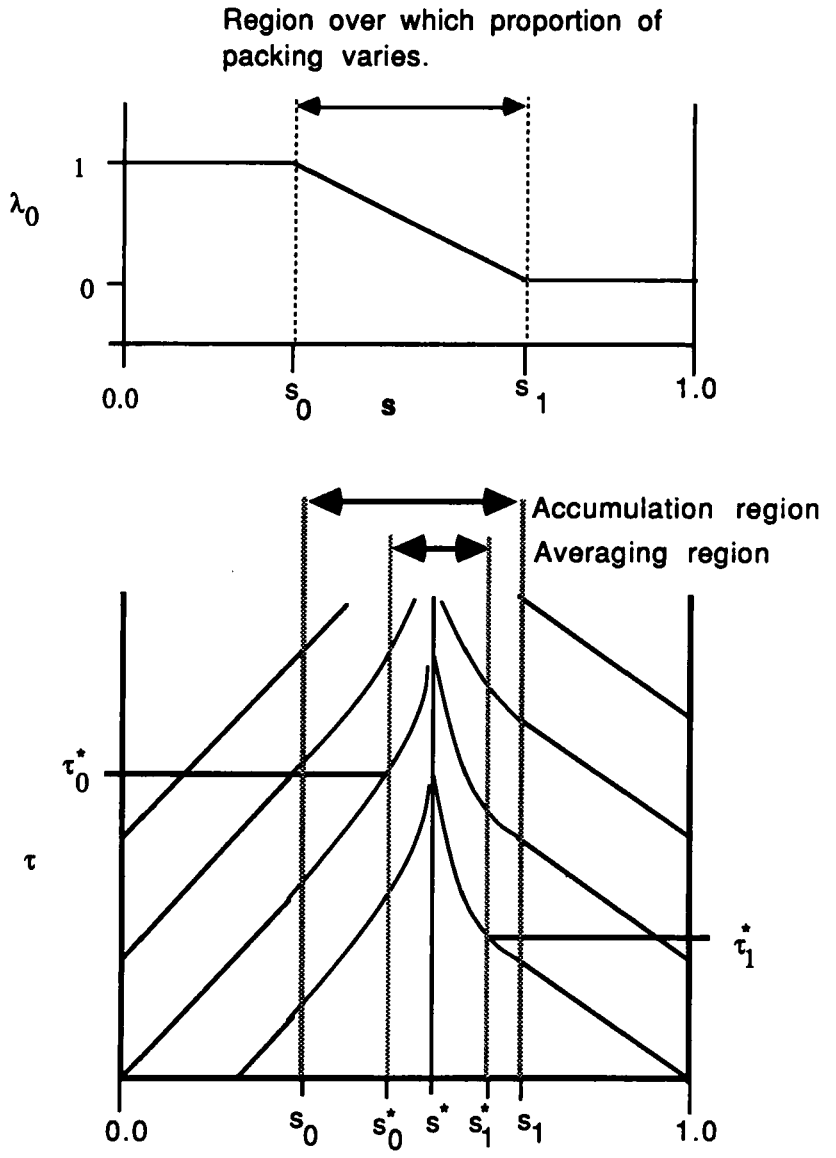

FIGURE 5
The characteristic plane for the accumulation conditions.

We are interested in calculating an average concentration of accumulated solute near s*. For this purpose, we define a region of integration of width $\Delta s^* = s_1^* - s_o^*$, centered about s* which we will use to do a mass balance in the interfacial zone (see Figure 5). Note that Δs^* is not necessarily equal to $s_1 - s_o$, in fact it is possible for Δs^* to be equal to, greater than, or less than $s_1 - s_o$. The size of region $s_1 - s_o$ depends entirely on how the column is packed. For the case considered up to this point where the bed goes from 100% polyacrylamide to 100% agarose at a very sharp interface the size of this region is very small. However, for the case where the column is packed so that the proportion of polyacrylamide to agarose varies throughout the length of the column the size of this region can be as large as the length of the column. The size of the averaging region depends upon the nature of the spreading due to diffusion and mass transfer.

It is clear that the band width of the averaging region will vary as concentration varies, however if Δs^* is taken large enough it will always include all the protein of interest for reasonable or practically achievable concentration increases. In this analysis Δs^* times the column area is the volume of column that is sampled in order to measure the amount of accumulated protein in the interfacial zone.

We now proceed with the calculation of the time variations of this concentration under varying operating conditions. Equations (23) lead to a differential equation for the concentration as a function of s which can be written as

$$\frac{dC}{d\omega} = \frac{-C\mu}{1 + \mu\,(1+\alpha(s)\,\Phi(s))} \frac{d[\alpha(s)\,\Phi(s)]}{d\omega} \tag{29}$$

The special form of this equation allows considerable simplification in the integration along a characteristic curve. Separating variables, an equation is obtained for C as a function of α and Φ

$$\frac{dC}{C} = - \frac{\mu d\,[\alpha(s)\,\Phi(s)]}{1 + \mu\,(1+\alpha(s)\,\Phi(s))} \tag{30}$$

This equation also has a discontinuity at $s = s^*$. Therefore we can integrate along the characteristics from either side of s* to the edges of the zone Δs^*. Integration along the characteristic from the upstream side of the accumulation zone, i.e. $s < s^*$, gives

$$C(s) = C_L \frac{(1 + \mu (1+\alpha_L \Phi_L))}{1 + \mu (1+\alpha(s) \Phi(s))} \tag{31}$$

for all $s \leq s_o^*$; $s_o^* < s^*$. Here C_L, Φ_L, and α_L are given by values at the boundary $s = 0$ for all $\tau > 0$ and at the initial state $\tau = 0$ for all $s \leq s_o^*$; i.e. at the origin of each characteristic curve.

Integration of equation (30) on the downstream side ($s > s^*$) similarly leads to

$$C(s) = C_R \frac{(1 + \mu (1 + \alpha_R \Phi_R))}{1 + \mu (1 + \alpha(s) \Phi(s))} \tag{32}$$

for all $s \geq s_1^*$; $s_1^* > s^*$. Here again C_R, Φ_R and α_R are given by values at the boundary $s = 1$ for all $\tau > 0$ and at the initial state $\tau = 0$ for all $s \geq s_1^*$. Given equations for the concentration as a function of position along the characteristics, we are in a position to calculate the accumulation. We separate the results into unsteady and steady-state modes of operation.

Unsteady-State Accumulation

A mass balance in the accumulation zone $\Delta s^* = s_1^* - s_o^*$ can be carried out by integrating equation (21) from s_o^* to s_1^*

$$\frac{\partial}{\partial \tau} \int_{s_o^*}^{s_1^*} [1 + \alpha(s)(1 + K(s))] C ds = - C(s_1^*)[1 + \mu(1 + \alpha(s_1^*) \Phi(s_1^*))]$$

$$+ C(s_o^*) [1 + \mu (1 + \alpha (s_o^*) \Phi(s_o^*))] \tag{33}$$

An average concentration C^* in the accumulation zone can be defined by the relation

$$[1 + \alpha(s^*)(1 + K(s^*))]\, C^* \equiv \frac{1}{\Delta s^*} \int_{s_o^*}^{s_1^*} [1 + \alpha(s)(1 + K(s))] Cds \qquad (34)$$

where $\alpha(s^*)$ and $K(s^*)$ are the values of α and K at $s = s^*$. Using the definition in equation (34), we can write equation (33) for the concentration C^* as

$$\Delta s^* \frac{dC^*}{d\tau} = + C(s_o^*) \frac{[1+\mu(1+\alpha(s_o^*)\,\Phi(s_o^*))]}{1 + \alpha(s^*)(1 + K(s^*))}$$

$$- C(s_1^*) \frac{[1 + \mu(1 + \alpha(s_1^*)\,\Phi(s_1^*))]}{1 + \alpha(s^*)(1 + K(s^*))} \qquad (35)$$

The quantity C^* is a direct measure of the concentration of accumulated solute in the sampling zone Δs^*.

Applying equation (31) at s_o^* and equation (32) at s_1^*, and substituting into equation (35) results in

$$\Delta s^* \frac{dC^*}{d\tau} = C_L \frac{1 + \mu(1 + \alpha_L \Phi_L)}{1 + \alpha(s^*)(1 + K(s^*))} - C_R \frac{1 + \mu(1 + \alpha_R \Phi_R)}{1 + \alpha(s^*)(1 + K(s^*))} \qquad (36)$$

In general C_L and C_R are specified functions dependent on the boundary and initial conditions. They can be functions of time at the boundaries and they can be functions of position at the initial time.

The two common cases are

$$\begin{aligned} &C_L = C_R = 1 \quad \text{at } \tau = 0 \text{ for all s excluding } \Delta s^* \\ &C_L = 1 \text{ for all } \tau > 0 \text{ and } s = 0 \\ &C_R = 0 \text{ for all } \tau > 0 \text{ and } s = 1 \\ &C^* = 1 \text{ at } \tau = 0 \text{ within } \Delta s^* \end{aligned} \qquad (37)$$

and

$$C_L = C_R = 0 \text{ at } \tau = 0 \text{ for all s excluding } \Delta s^*$$
$$C_L = 1 \text{ for all } \tau > 0 \text{ and } s = 0$$
$$C_R = 0 \text{ for all } \tau > 0 \text{ and } s = 1$$
$$C^* = 0 \text{ at } \tau = 0 \text{ within } \Delta s^* \tag{38}$$

The first case would involve starting the column with a uniform concentration in the column equal to the feed concentration. We will call this case the initially loaded column case. The second case would involve starting the column with no species initially present. This will be referred to as the initially empty column case. Both of these cases would give rise to step changes in the concentration reaching the accumulation zone at some time after the start.

Referring back to Figure 5 it is clear that the characteristics emanating from $\tau = 0$, $s = 0$ will reach the boundary s_o^* of the Δs^* region at some time τ_o^*. Similarly the characteristic from $\tau = 0$, $s = 1$ reaches s_1^* at τ_1^*. Prior to τ_o^* the characteristics that reach s_o^* all emanate from the initial state of the bed on the upstream side for $\tau = 0$, $0<s<s_o^*$. After τ_o^* the characteristics from the boundary at $s = 0$ $\tau > 0$ reach s_o^*. Similary prior to τ_1^* the characteristics that reach s_1^* all emanate from $\tau = 0$, $1>s>s_1^*$, and after τ_1^*, they emanate from $s = 1$, $\tau > 0$.

The times τ_o^* and τ_1^* can be determined from the integration of equation (24)

$$\tau_o^* = \int_o^{s_o^*} \frac{1+\alpha(s)(1+K(s))}{1+\mu(1+\alpha(s)\Phi(s))}\,ds \tag{39}$$

$$\tau_1^* = \int_1^{s_1^*} \frac{1+\alpha(s)(1+K(s))}{1+\mu(1+\alpha(s)\Phi(s))}\,ds \tag{40}$$

The boundary and initial condition in equations (37) and (38) can then be written in terms of the times τ_o^* and τ_1^* for the initially loaded case

$$C^* = 1 \text{ at } \tau = 0$$
$$C_L = 1 \text{ for all } \tau$$

$$C_R = 1 \text{ for all } \tau_1^* \geq \tau > 0$$
$$C_R = 0 \text{ for all } \tau > \tau_1^* \tag{41}$$

while for the initially empty column case they are

$$C^* = 0 \text{ at } \tau = 0$$
$$C_L = 1 \text{ for all } \tau \geq \tau_o^*$$
$$C_L = 0 \text{ for all } \tau < \tau_o^*$$
$$C_R = 0 \text{ for all } \tau \tag{42}$$

One further point prior to solving equation (36) for the two cases of boundary and initial conditions given above is that since the terms $\alpha_L\Phi_L$ and $\alpha_R\Phi_R$ are functions of position at τ=0 and $s_o < s < s_o^*$ and $s_1^* < s < s_1$, they will also be function of time at s_o^* and s_1^* for the time intervals of $\tau<\tau_o^*$ and $\tau<\tau_1^*$ respectively. This is seen in Figure 5 because the positional dependence at τ=0 is transformed into a time dependence at s_o^* and s_1^* as the characteristics from τ=0 migrate to the vertical lines at s_o^* and s_1^*.

In order to get $\alpha_L\Phi_L$ and $\alpha_R\Phi_R$ as functions of time it is necessary to first determine the relationship between time and distance along the characteristics from each side of the interface. To get $\alpha_L\Phi_L$ it is necessary to solve for τ from the intergral

$$\tau = \int_o^s \frac{1+\alpha(s)(1+K(s))}{1+\mu(1+\alpha(s)\Phi(s))}\, ds \equiv g(s) \text{ for } s_o < s < s_o^* \tag{43}$$

Once τ is known as a function of s, it is possible to calculate $\alpha_L\Phi_L$ from the relation

$$\alpha_L\Phi_L = \alpha_L(g^{-1}(\tau))\,\Phi_L(g^{-1}(\tau)) \tag{44}$$

This will give $\alpha_L\Phi_L = \alpha_L(\tau)\Phi_L(\tau)$ to use in equation (36). It is similarly necessary to find

$$\tau = \int_{1}^{s} \frac{1 + \alpha(s)(1+K(s))}{1 + \mu(1+\alpha(s)\Phi(s))} ds \equiv h(s) \quad \text{for } s_1 > s > s_1^* \tag{45}$$

to get $\tau=h(s)$ and thus

$$\alpha_R \Phi_R = \alpha_R (h^{-1}(\tau))\Phi_R (h^{-1}(\tau)) \tag{46}$$

This procedure will be unnecessary wherever the averaging region Δs^* includes the whole region Δs over which the properties vary. However, it will be necessary to follow this complete procedure when considering the case where the proportion of packing varies continuously down the length of the column; i.e. where Δs is large. An example will be given for the multicomponent case of two proteins.

Continuous Removal

Under steady-state conditions, material can be removed at a constant rate from the accumulation zone Δs^*. In this case, the mass balance over this region is given by

$$\Delta s^* \frac{dC^*}{d\tau} = C_L \frac{(1+\mu(1+\alpha_L \Phi_L))}{1+\alpha(s^*)(1+K(s^*))} - C_R \frac{(1+\mu(1+\alpha_R \Phi_R))}{1+\alpha(s^*)(1+K(s^*))}$$

$$- \frac{QC^*}{1 + \alpha(s^*)(1 + K(s^*))} \tag{47}$$

where the dimensionless flow rate, Q, is given by the ratio of the flow rate of sample removed from the bed, Q_R, to the total flow rate through the bed

$$Q = \frac{Q_R}{v\varepsilon a} \tag{48}$$

Here a is the column area. It will generally be assumed that Q is much less than one, and thus no correction will be made for the flow in the column downstream of the removal point.

Equation (47) can be solved subject to the boundary condition in equations (41) and (42) and with the expressions in equations (44) and (46) for $\alpha_L\Phi_L$ and $\alpha_R\Phi_R$.

Examples

Solutions to both the unsteady-state accumulation and the continuous removal processes are presented in the next section for a linear functional form for $\lambda(s)$. A linear function for the dependence of the relative proportion of packing on position in the bed will be assumed in order to illustrate the primary feature of the separation process. The equations for λ and β' for a particular species become

$$\lambda_o = 1 - \left(\frac{s - s_0}{s_1 - s_o}\right) \quad \text{for } s_1 > s > s_o$$

$$\lambda_1 = 1 - \lambda_o$$

$$\beta' = \beta_o + (\beta_1 - \beta_o)\left(\frac{s - s_o}{s_1 - s_o}\right)$$

$$\lambda_o = 1\,, \quad \beta' = \beta_i{}' = \beta_o \quad \text{for } s < s_o$$

$$\lambda_o = 0\,, \quad \beta' = \beta_i{}' = \beta_1 \quad \text{for } s > s_1 \tag{49}$$

In terms of the variable $\alpha(s)$ in equation (20)

$$\alpha(s) = \delta_1 + \delta_2 s \quad \text{for } s_1 > s > s_o$$

$$\alpha = \delta_1 + \delta_2 s_o = \alpha_o \quad \text{for } s < s_o$$

$$\alpha = \delta_1 + \delta_2 s_1 = \alpha_1 \quad \text{for } s > s_1 \tag{50}$$

Here, the quantities δ_1 and δ_2 are defined by

$$\delta_1 = \left[\beta_o - s_o\frac{(\beta_1\beta_0)}{(s_1 - s_o)}\right]\left(\frac{1-\varepsilon}{\varepsilon}\right)$$

$$\delta_2 = \left(\frac{\beta_1 - \beta_0}{s_1 - s_o}\right)\left(\frac{1-\varepsilon}{\varepsilon}\right) \tag{51}$$

The equation for $\Phi(s)$ is given by

$$\Phi = \phi_o + (s - s_o)\left(\frac{\phi_1 - \phi_o}{s_1 - s_o}\right) \text{ for } s_1 > s > s_o$$
$$\Phi = \phi_o \text{ for } s < s_o$$
$$\Phi = \phi_1 \text{ for } s > s_1 \tag{52}$$

Therefore

$$\Phi(s) = \delta_3 + \delta_4 s \quad \text{for} \quad s_1 > s > s_o$$
$$\Phi(s) = \delta_3 + \delta_4 s_o = \phi_o \quad \text{for} \quad s < s_o$$
$$\Phi(s) = \delta_3 + \delta_4 s_1 = \phi_1 \quad \text{for} \quad s > s_1 \tag{53}$$

where

$$\delta_3 = \phi_o - s_o\left(\frac{\phi_1 - \phi_o}{s_1 - s_o}\right)$$
$$\delta_4 = \left(\frac{\phi_1 - \phi_o}{s_1 - s_o}\right) \tag{54}$$

The equations for K(s) are given as

$$K(s) = \delta_5 + \delta_6 s \quad \text{for} \quad s_1 > s > s_o$$
$$K(s) = \delta_5 + \delta_6 s_o = \kappa_o \quad \text{for} \quad s < s_o$$
$$K(s) = \delta_5 + \delta_6 s_1 = \kappa_1 \quad \text{for} \quad s > s_1 \tag{55}$$

where

$$\delta_5 = \kappa_o - s_o\left(\frac{\kappa_1 - \kappa_o}{s_1 - s_0}\right)$$

$$\delta_6 = \left(\frac{\kappa_1 - \kappa_o}{s_1 - s_o} \right)$$

For simplicity, it is assumed that $\Delta s^* = s_1 - s_o$, and thus the region that defines C*, coincides with the zone where α and Φ change. In this case α and Φ will be constant outside of Δs^*. Therefore $\alpha_L = \alpha_o$, $\Phi_L = \phi_0$ and $\alpha_R = \alpha_1$, $\Phi_R = \phi_1$ and equations (36) and (47) can be integrated directly with the boundary and initial conditions in equations (41) and (42). Note that this will not be the case for the multicomponent case considered in a following section.

The solution for the case of no withdrawal from the column, equation (41), and a uniform initial concentration in the column, boundary condition (46), is

$$C^* = 1 + \frac{\tau}{\Delta s^* (1 + \alpha(s^*)(1 + K(s^*)))} [\mu(\alpha_o \phi_o - \alpha_1 \phi_1)] \quad \text{for all } \tau \le \tau_1^*$$

$$C^* = C^*(\tau_1^*) + \frac{(\tau - \tau_1^*)}{\Delta s^*(1+\alpha(s^*)(1+K(s^*)))} [1+\mu(1+\alpha_o \phi_o)] \quad \text{for all } \tau > \tau_1^* \qquad (56)$$

where

$$\tau_1^* = \frac{(1+\alpha_1(1+K_1))}{1+\mu(1+\alpha_1)} (s_1 - 1)$$

For the case of no withdrawal from the column and no solute in the column at time τ=0, boundary condition (42), the result is

$$C^* = 0 \quad \text{for all} \quad \tau \le \tau_o^*$$

$$C^* = \frac{(\tau - \tau_o^*)}{\Delta s^*(1+\alpha(s^*)(1+K(s^*)))} [1+\mu(1+\alpha_o \phi_o)] \quad \text{for all} \quad \tau > \tau_o^* \qquad (57)$$

where

$$\tau_o^* = \frac{(1 + \alpha_o(1 + K_o))\, s_o}{1 + \mu\,(1 + \alpha_o\phi_o)}$$

The solution for the case of continuous removal from the interface, equation (47), and uniform initial concentration in the column, boundary condition (41), is

$$C^* = \frac{\mu}{Q}(\alpha_o\phi_o - \alpha_1\phi_1) +$$

$$\exp\left(\frac{-Q\tau}{\Delta s^*(1+\alpha(s^*)(1+K(s^*)))}\right)\left(1-\mu\frac{(\alpha_o\phi_o - \alpha_1\phi_1)}{Q}\right) \quad \text{for all } \tau < \tau_1^* \qquad (58)$$

$$C^* = \frac{1 + \mu(1+\alpha_o\phi_o)}{Q} +$$

$$\exp\left(\frac{-Q(\tau - \tau_1^*)}{\Delta s^*(1+\alpha(s^*)(1+K(s^*)))}\right)\left(C^*(\tau_1^*) - \frac{1+\mu(1+\alpha_o\phi_o)}{Q}\right) \quad \text{for all } \tau > \tau_1^*$$

For the case of an initialy empty column and continuous removal the solution is

$$C^* = 0 \quad \text{for all} \quad \tau \le \tau_o^*$$

$$C^* = \frac{1 + \mu(1+\alpha_o\phi_o)}{Q}\left(1 - \exp\left[\frac{-Q(\tau-\tau_1^*)}{\Delta s^*(1+\alpha(s^*)(1+K(s^*)))}\right]\right) \quad \text{for all } \tau > \tau_o^* \qquad (59)$$

Unsteady-State Accumulation

Using the parameters $\beta_1 = 1$, $\beta_0 = 0$, $\phi_1 = 1$, $\phi_0 = 0$, $K_0 = 0$, and $K_1 = K_1$ the value of α_0 goes to zero and that of α_1 goes to $(1-\varepsilon)/\varepsilon$ by equations (50) and (51). In addition Φ_0 goes to zero and Φ_1 goes to 1 by equations (53) and (54). Furthermore, using equation (28)

$$1 + \alpha(s^*)(1+K(s^*)) = 1 + K_1\frac{1-|\mu|}{|\mu|} + \sqrt{\frac{1-|\mu|}{|\mu|}\frac{1-\varepsilon}{\varepsilon}} \tag{60}$$

Equation (56) for the initially loaded case can be simplified to

$$C^* = 1 + \left[\frac{\tau}{\Delta s^*(1+\alpha(s^*)(1+K(s^*)))}\right]\left(|\mu|\left(\frac{1-\varepsilon}{\varepsilon}\right)\right) \quad \text{for all } \tau \le \tau_1^* \tag{61}$$

$$C^* = \frac{(\tau-\tau_1^*)}{\Delta s^*(1+\alpha(s^*)(1+K(s^*))}[1-|\mu|] + C^*(\tau^*) \quad \text{for all } \tau > \tau_1^*$$

$$\text{where } \tau_1^* = (s_1 - 1)\frac{(1+(1-\varepsilon)K_1)/\varepsilon}{1-|\mu|/\varepsilon}$$

Equation (57) for the initially empty case can be simplified to

$$C^* = 0 \quad \text{for all} \quad \tau \le \tau_0^* \tag{62}$$

$$C^* = \frac{[\tau-\tau_0^*][1-|\mu|]}{\Delta s^*(1+\alpha(s^*)(1+K(s^*)))} \quad \text{for all} \quad \tau > \tau_0^*$$

$$\text{where } \tau_0^* = \frac{s_0}{1-|\mu|}$$

Note that $1 > |\mu| > \varepsilon$ and that $s_1 = \Delta s^* + s_0$.

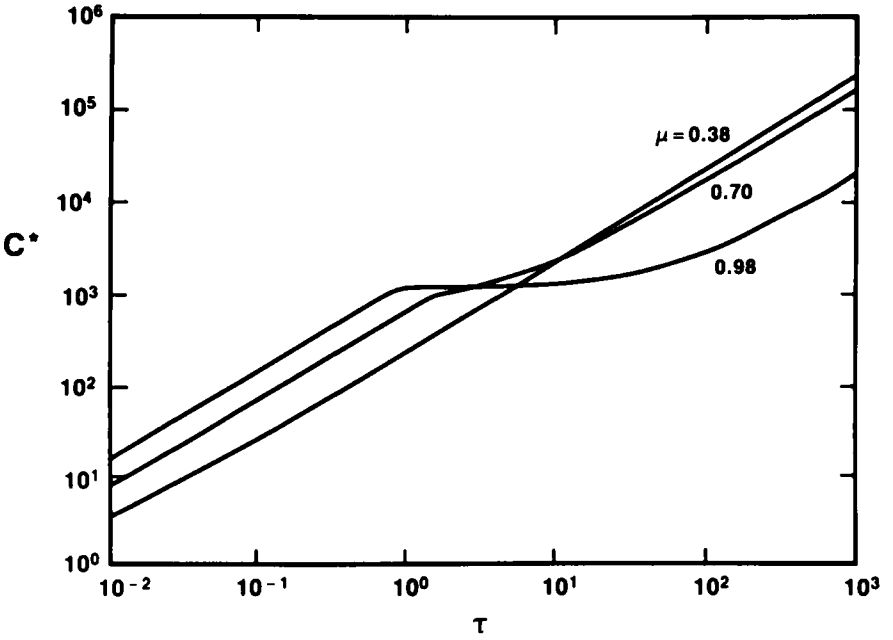

FIGURE 6
Accumulation for an initially loaded bed withjout product removal.

Figure 6 illustrates the concentration increase with time for the case where the bed was initially loaded with protein and neglecting adsorption; i.e. setting K = 0 and $\Delta s^* = .001$. The parameter $|\mu|$ is seen to affect the results very strongly. This parameter is the ratio of the electrical migration to the convective flow. When $|\mu|$ is close to 1, its upper limit for accumulation in the bed, the rate of increase in concentration is very rapid for small τ. This is due to the fact that material is going to the accumulation zone from both sides of the bed. In the limit when $|\mu| = 1.0$ after time τ_1^* no more accumulation would be observed because all the protein from the right side of the bed would have reached the accumulation zone, but the value of $|\mu|$ is too large to allow the protein to move through the left side of the bed.

As $|\mu|$ decreased the initial rate of concentration increase gets smaller. However, at large times the largest rate of increase is found for $|\mu| = 0.38$. This is close to the

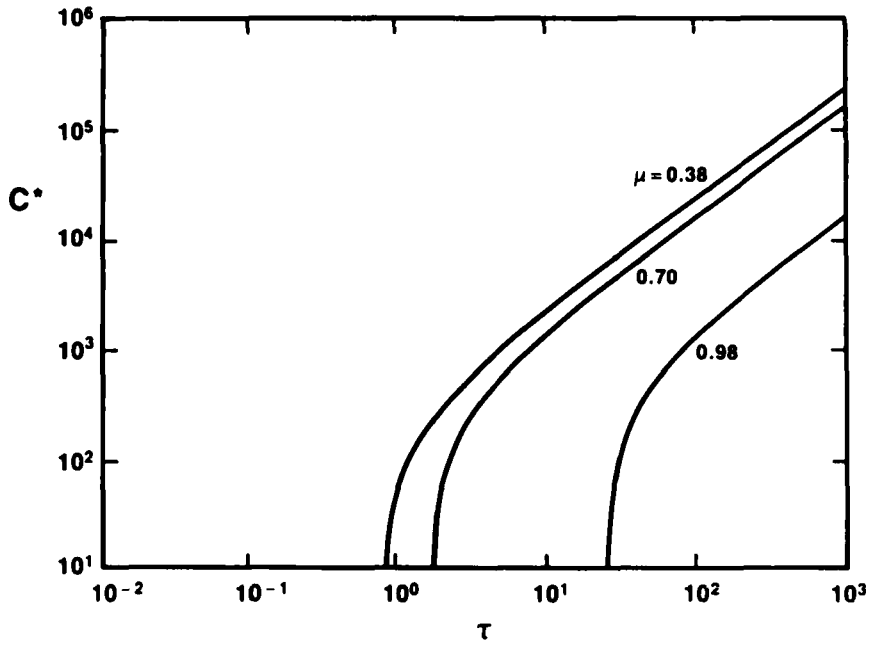

FIGURE 7
Accumulation for an initially empty bed without product removal.

lower limit for the range of $|\mu| = \varepsilon$. Thus, for the operation of an initially loaded bed it may be advantageous to vary $|\mu|$ from 1.0, the upper limit for accumulation, at small τ to keep the concentration increase large for all τ. For $|\mu|$ close to 1.0, the electrical migration rate is larger in relation to the convective flow than for $|\mu|$ close to the lower limit of ε. In this initially loaded case the protein would thus move more rapidly back to the interface in the downstream, i.e. agarose, section of the column when $|\mu|$ is larger. However, once this agarose section of the column is depleted of protein it would be better to operate with a lower value of $|\mu|$ to facilitate the motion of the protein in the polyacrylamide section of the column.

Figure 7 illustrates the concentration increase with τ for the case where the column is initially empty. The concentrations are all zero prior to $\tau=\tau_o^*$. Above $\tau=\tau_o^*$ the concentrations increase very rapidly with $|\mu| = .38$. Under these

circumstances it appears that it would be advantageous to start operation with $|\mu|$ near 0.38, i.e. near the lower limit of ε.

At very large τ the concentration for the initially empty bed approach those of the initially loaded bed, however it is generally not desirable to have to wait for these long times, and thus an initially loaded bed appears to be much more useful.

Continuous Removal

Again using $\beta_o = 0$, $\beta_1 = 1$, $\phi_1 = 1$, and $\phi_o = 0$ equation (58) for the case of an initially loaded bed can be simplified to

$$C^* = \frac{|\mu|}{Q}\left(\frac{1-\varepsilon}{\varepsilon}\right) + \exp\left[\frac{-Q\tau}{\Delta s^*(1+\alpha(s^*)(1+K(s^*)))}\right]\left[1-\frac{|\mu|}{Q}\left(\frac{(1-\varepsilon)}{\varepsilon}\right)\right] \text{ for all } \tau \le \tau_1^* \qquad (63)$$

$$C^* = \frac{1 - |\mu|}{Q} +$$

$$\exp\left[\frac{-Q}{\Delta s^*(1+\alpha(s^*)(1+K(s^*)))}\left(\tau-\tau_1^*\right)\right]\left[C^*(\tau_1^*) - \frac{1-|\mu|}{Q}\right] \quad \text{for all } \tau > \tau_1^*$$

$$\text{where } \tau_1^* = (s_1 - 1)\frac{(1+(1-\varepsilon)K_1)/\varepsilon}{1-|\mu|/\varepsilon}$$

Equation (59) for the case of an initially empty bed can be simplified to

$$C^* = 0 \quad \text{for all} \quad \tau \le \tau_o^* \qquad (64)$$

$$C^* = \frac{1-|\mu|}{Q} + \exp\left[\frac{-Q}{\Delta s^*(1+\alpha(s^*)(1+K(s^*)))}\left(\tau-\tau_o^*\right)\right]\left[-\frac{1-|\mu|}{Q}\right] \text{ for all } \tau > \tau_o^*$$

$$\text{where } \tau_o^* = \frac{s_o}{1 - |\mu|}$$

Figure 8 illustrates the concentration increase with time for the initially loaded column case for a constant Q without adsorption where $\Delta s^* = .001$ and $Q = .001$.

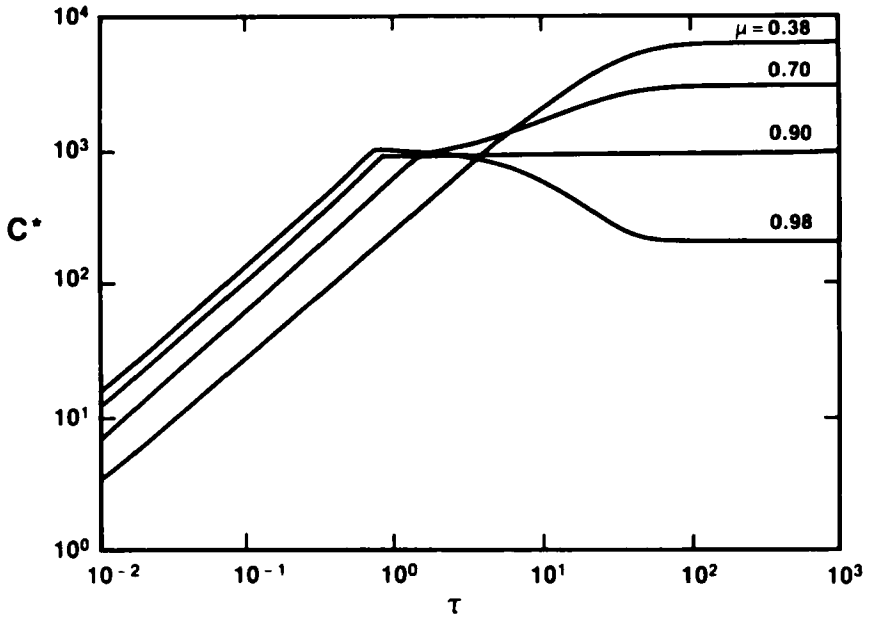

FIGURE 8
Accumulation for an initially loaded bed with product sidestream removal.

Large |μ| values (near one) give rapid increases in concentration at small τ, however the final steady-state concentrations are larger for the smaller |μ|. There is a critical |μ|, shown in this figure as 0.90, above which the concentration decreases when the time becomes greater than τ_1^*. Although the concentrations at steady-state are larger for the small |μ|, it takes longer to reach those steady states. The critical value of |μ| = 0.90 thus represents an optimum whereby the steady-state is reached faster than for other |μ| at the same Q and s_0. The value of |μ| at this critical point is given by the solution to the equation

$$C^*(\tau_1^*) = \frac{1 - |\mu|_{crit}}{Q} \tag{65}$$

where $C^*(\tau_1^*)$ is given by the first equation in (63) applied at $\tau=\tau_1^*$.

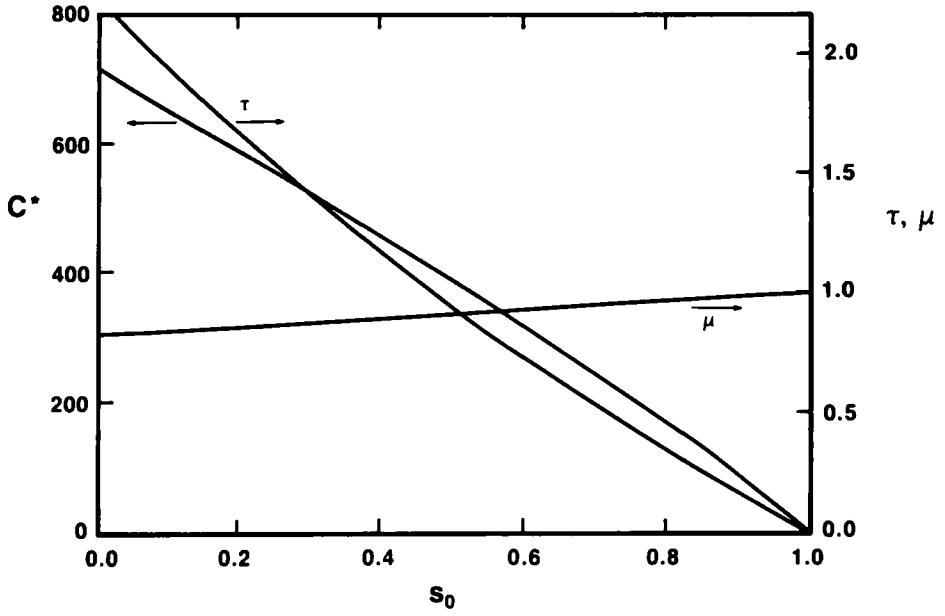

FIGURE 9
Design curves for the case of continuous side stream removal at the critical μ.

Figure 9 illustrates the variation in the optimum |μ| with the value of s_0. This figure also shows the effect of s_0 on C_s*, the steady-state concentration achievable at that |μ| and τ_1* the time required to reach the steady-state. The s_0 is a measure of the proportion of the total bed that is made up of polyacrylamide. The largest concentration increase occur at the smallest s_0 and the smallest |μ|, however it takes longer to reach steady-state at this value of s_0.

Figure 10 illustrates the effect of Q on the concentration increase for a given |m|. It is clear that the smaller Q the faster the initial concentration increases and the higher the final steady-state concentration. When Q is too large it tends to reduce the concentration after time to* because after this time the concentration reaching the Ds* region decreases as the right had side of the bed is depleted.

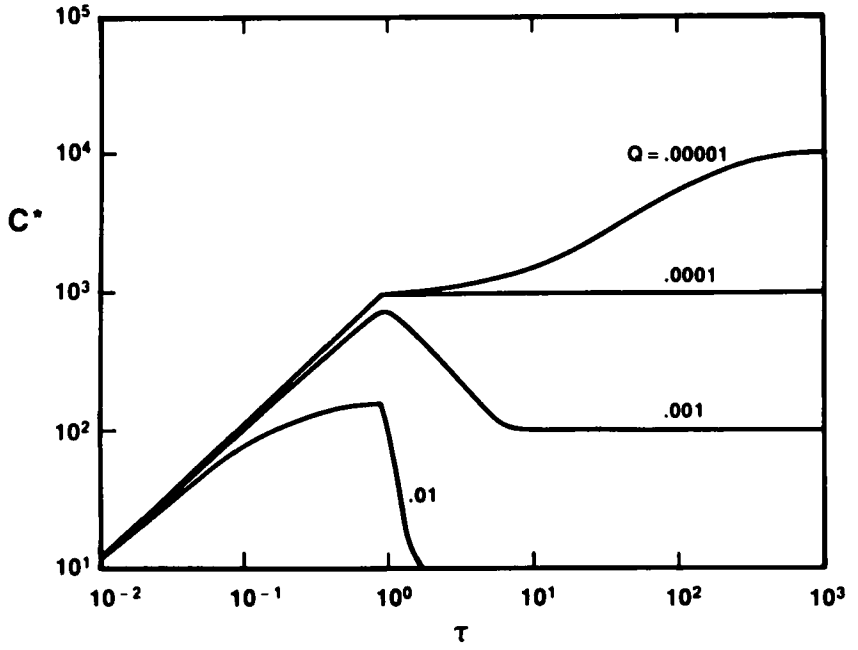

FIGURE 10
The effect of the withdrawal rate on the concentration increase with time.

Figure 11 illustrates the effect of Q for various |m| on the steady-state concentration. This again shows that large Q will deplete the concentration, however for a given C* a smaller |m| will require a larger Q.

An initially empty bed gives the same final steady-state as the initially full bed as is seen by comparing Figure 12 with Figure 8. The steady-states are reached at about the same time except with the critical value of |m| = .90. The steady-state concentration for the initially loaded bed is reached at a t close to one where for the initially empty bed it is not reached until t is close to 70. This clearly shows the advantage of operating with an initially loaded bed at the critical |m|.

Figure 13 illustrates the effect of adsorption for the continuous removal case. It is seen that as the adsorption constant K increases, the time required to reach

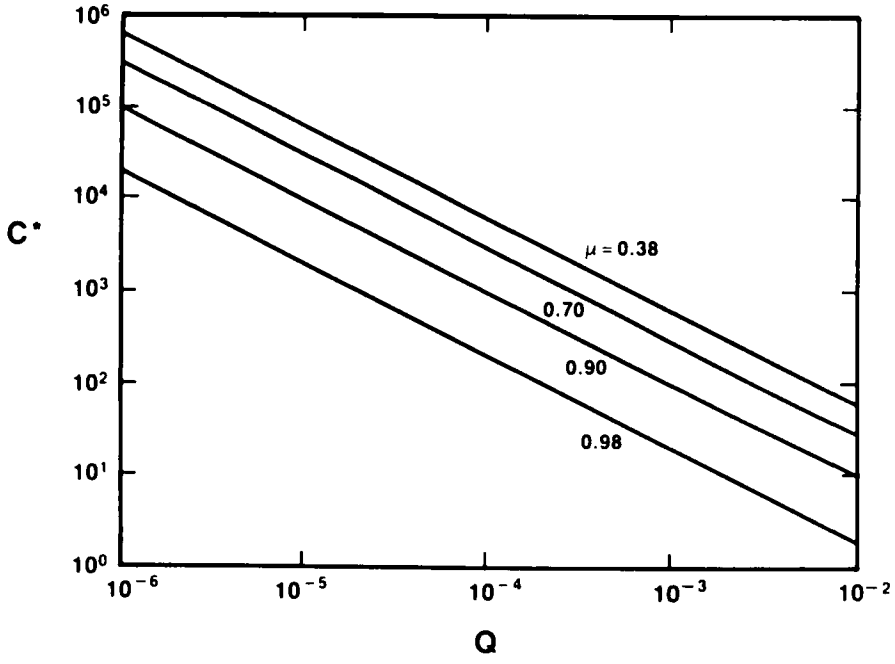

FIGURE 11
The effect of the withdrawal rate on the steady-state concentration.

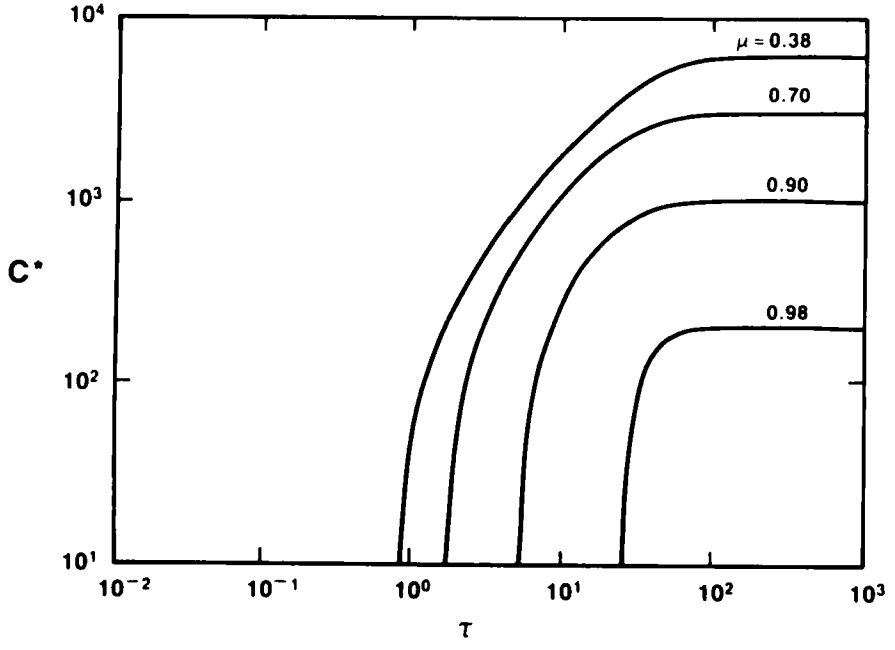

FIGURE 12
Accumulation for an initially empty bed with continuous removal.

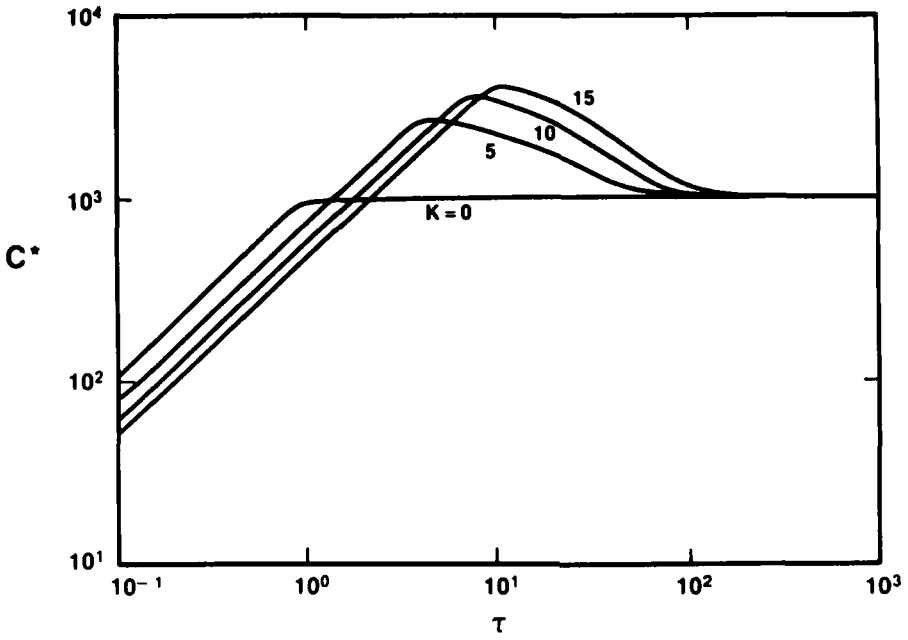

FIGURE 13
The effect of adsorption for the case of continous sidestream removal.

steady-state increases, and the final steady-state concentrations are identical to the K = 0 case. In addition, it is seen that the concentration rise is at first lower for the larger adsorption, but it reaches a maximum, and thereafter drops steadily to the same steady-state concentration.

Multicomponent Separation

If a column is designed so that the first component will accumulate, it is necessary to determine under what conditons another component will also accumulate in the column. Equation (26) for the first component is given as

$$\frac{1}{\beta_{11}\phi_{11}\dfrac{1-\varepsilon}{\varepsilon}+1} < |\mu_1| < \frac{1}{\beta_{10}\phi_{10}\dfrac{1-\varepsilon}{\varepsilon}+1} \tag{66}$$

In order for another k species to accumulate it is necessary for

$$\frac{1}{\beta_{k1}\phi_{k1}\frac{1-\varepsilon}{\varepsilon}+1} < |\mu_k| < \frac{1}{\beta_{ko}\phi_{ko}\frac{1-\varepsilon}{\varepsilon}+1} \tag{67}$$

From the definition of $|\mu_1|$ and $|\mu_k|$ in equation (20)

$$F\,|I/\Omega|\,/v = \frac{|\mu_1|}{|u_1|} = \frac{|\mu_k|}{|u_k|} \tag{68}$$

therefore equation (67) becomes

$$\frac{\left|\frac{u_1}{u_k}\right|}{\beta_{ko}\phi_{ko}\frac{1-\varepsilon}{\varepsilon}+1} > |\mu_1| > \frac{\left|\frac{u_1}{u_k}\right|}{\beta_{k1}\phi_{k1}\frac{1-\varepsilon}{\varepsilon}+1} \tag{69}$$

Figure 14 illustrates the range of parameters over which both components will be collected in the bed. The crossed area between the two lines defines the range of $|\mu_1|$ and $|u_1/u_k|$ that allow species k to accumulate. In order to narrow the range of $|\mu|$ that will allow only one protein to accumulate in the column it is thus necessary to make β_{ko} close to β_{k1}.

It is important to note that in a process where species k is not initially accumulated in the bed it may be possible to accumulate species k at a later time if $|\mu_1|$ is varied by changing the current with time without concern for the effects shown in Figure 14.

For the single component case that we have discussed in the previous sections we have been primarily concerned with a sharp transition between the polyacrylamide gel particles and the agarose gel particles. For a column packed with such a sharp transition region any protein that accumulates will accumulate at the sharp interface. Thus, if a mixture of proteins is fed into the column with conditions within the hatched portion of Figure 14 all k proteins will be

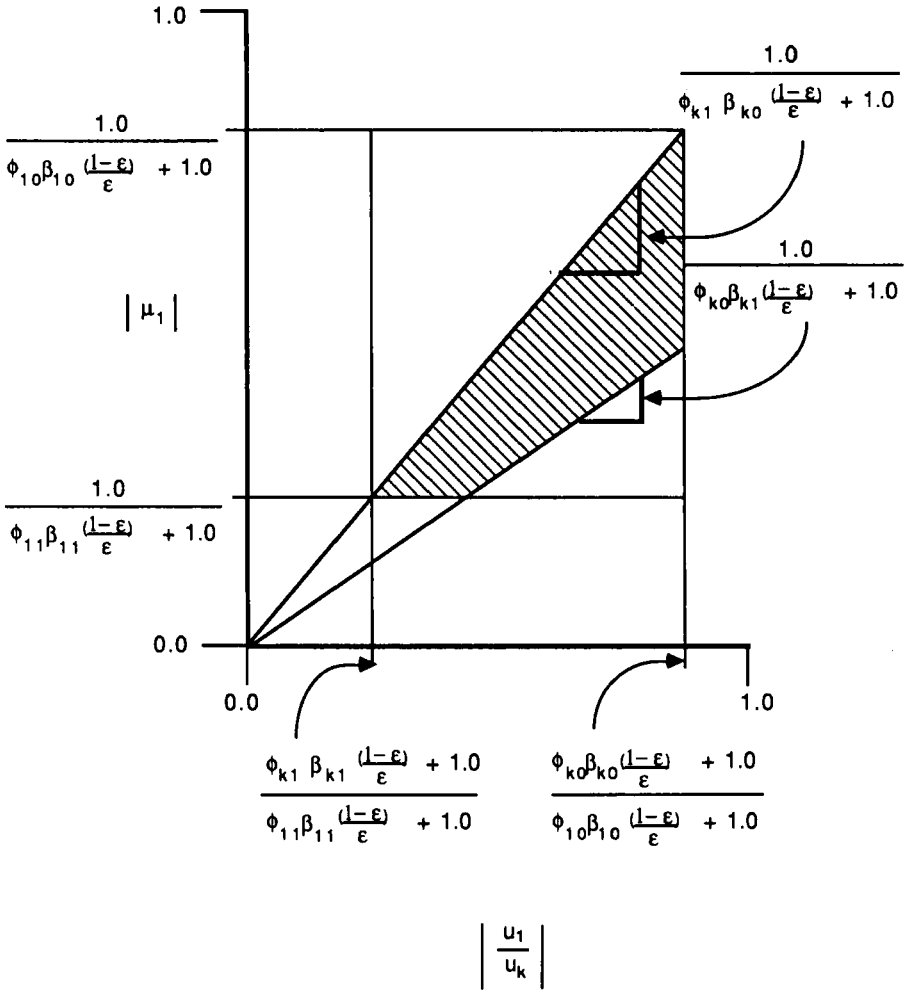

FIGURE 14
The criterion for the simultaneous accumulation of another k species with reference to the accumulation of species 1.

accumulated at the same sharp transition in the column. It would thus not be possible to further separate the proteins in this apparatus. However, if this transition region of variable porosity was spread out so that there was a continuous variation of porosity through the entire length of the column, it might be possible to improve the separation.

O'Farrell[1] packed a column with six sections of varying proportions of agarose and polyacrylamide particles. The first section contained 100% polyacrylamide, the next four sections contained relative proportions of 80/20, 60/40, 40/60, and 20/80 of polyacrylamide and agarose respectively, and the last section contained 100% agarose. He did not test the concept of separating several proteins with this mode of packing the column, although he did report that he was able to move the protein from one interface to another by small changes in the applied potential.

Our model can be easily extended to the case where the proportion of particles varies continuously down the length of the column. Figure 15 illustrates the difference between the packing variation in a narrow region and the variation over the length of the column. This represents a limiting case of O'Farrell's packing procedure described above. The limiting case would require an infinite number of sections with various proportions of packings. To account for this in our model it is necessary to make $\Delta s = s_1 - s_o$ large. Setting $\Delta s = 1$ gives the maximum variation down the column. The concentration profile of each protein will now have a different centroid given by s_k^*. The value of s_k^* for each protein is given by equation (28). In order to determine how far apart the centroids for each protein are it is necessary to use

$$s_1^* - s_k^* = (s_1 - s_o)\left[1 + \frac{\beta_{10}}{\beta_{10} - \beta_{11}} - \frac{\beta_{ko}}{\beta_{ko} - \beta_{k1}}\right]$$

$$+ (s_1 - s_o)\left[\sqrt{\varepsilon/(1-\varepsilon)}\left\{\frac{\sqrt{(1-|\mu_1|)/|\mu_1|}}{\beta_{10} - \beta_{11}} - \frac{\sqrt{(1-|\mu_k|)/|\mu_k|}}{\beta_{ko} - \beta_{k1}}\right\}\right] \qquad (70)$$

If the magnitude of the distance given by equation 70 is large enough so that the diffusional spreading does not cause the proteins to overlap, as shown in Figure 14, it would be possible to separate the kth protein from the first protein.

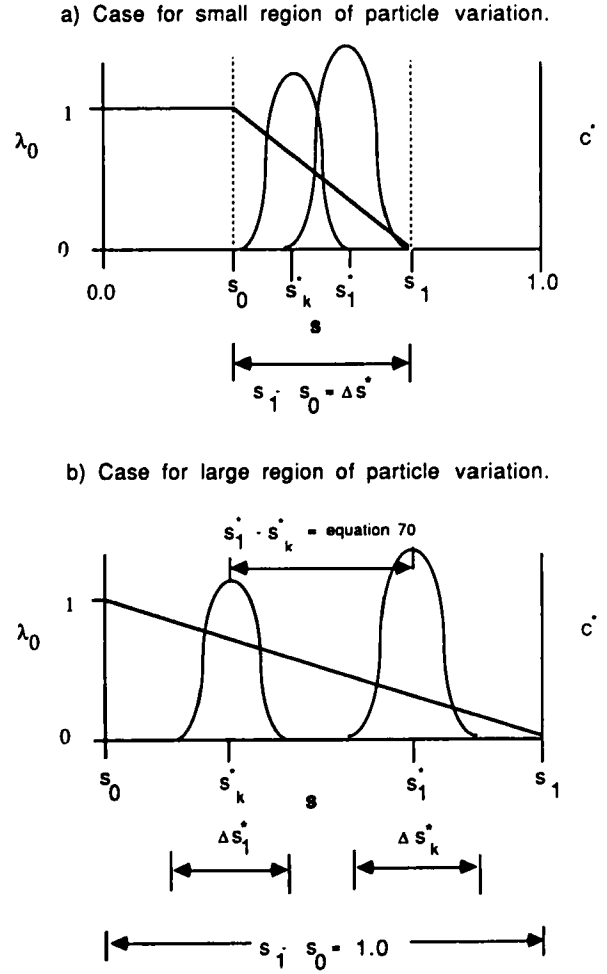

FIGURE 15
The effect of increasing the region of particle variation on the separation of two species.

As an example of the type of multicomponent separation possible we shall consider a two component case with $\Delta s = s_1 - s_o = 1$ where $s_1 = 1$ and $s_o = 0$. Furthermore, we shall neglect adsorption by letting $\kappa_1 = \kappa_2 = 0$, and we shall consider the case of no product withdrawal from the interface by letting $Q = 0$. In addition we let $\beta_{10} = 0$, $\beta_{20} = 0$, $\beta_{11} = 1$, $\beta_{21} = .5$, and $\varepsilon = .37$. We also let $\Delta s_1^* = \Delta s_o^* = 0.1$. From equation (52) $\Phi(s) = s$ and from equations (50) and (51) $\alpha(s) = s(1-\varepsilon)/\varepsilon$. The characteristics for the interval $0 < s < s_o^*$ are given by

$$\tau = \int_0^s \frac{1 + s(1-\varepsilon)/\varepsilon}{1-|\mu|(1 + (1-\varepsilon)/\varepsilon)}\, ds \tag{71}$$

The characteristics for the interval $1 > s > s_1^*$ are given by

$$\tau = \int_1^s \frac{1 + s\,(1-\varepsilon)/\varepsilon}{1-|\mu|(1 + (1-\varepsilon)/\varepsilon)}\, ds \tag{72}$$

From equation (28) the values of s^* and $\alpha(s^*)$ are given by

$$s^* = \sqrt{\frac{1-|\mu|}{|\mu|}\,\frac{\varepsilon}{1-\varepsilon}} \tag{73}$$

$$\alpha(s^*) = s^{*2}\frac{(1-\varepsilon)}{\varepsilon} \tag{74}$$

From equations (43) and (45) the functions g(s) and h(s) are given by

$$\tau = g(s) = \frac{1}{2|\mu|} \ln \frac{(s^*+s)^{(1-\alpha(s^*))/\alpha(s^*)}}{(s^* - s)^{1+\alpha(s^*))/\alpha(s^*)}}\, s^{*2} \quad \text{for } s_o^* > s > 0 \tag{75}$$

$$\tau = h(s) = \frac{1}{2|\mu|} \ln \left(\frac{s^* + s}{s^* + 1}\right)^{(1-\alpha(s^*))/\alpha(s^*)} \left(\frac{s^* - 1}{s^* - s}\right)^{(1+\alpha(s^*))/\alpha(s^*)} \text{ for } s_1^* < s < 1 \quad (76)$$

The accumulation criterion for species 1 and 2 are given by

$$1 > |\mu_1| > .37 \qquad 1 > |\mu_2| > .70$$

If, for example, we assume that the mobility in free solution of species 1 is half of the mobility of species 2 in free solution it is necessary for $0.5 > |\mu_1| > .37$ in order for both species to accumulate in the column. We let $|\mu_1| = .45$. Therefore $|\mu_2| = .90$. Thus,

s_1^*	= .847	s_2^*	= .255
$\alpha_1(s_1^*)$	= 1.22	$\alpha_2(s_2^*)$	= .111
s_{10}^*	= .797	s_{20}^*	= .205
s_{11}^*	= .897	s_{21}^*	= .305
τ_{11}^*	= 2.27	τ_{21}^*	= 11.4
τ_{10}^*	= 5.59	τ_{20}^*	= 11.6

For the case of an initially empty column the concentration increases for the two species are given by

$C_1^* = 2.48\ (\tau - 5.59)$ at $s = s_1^* = .847$

$C_2^* = 0.9\ (\tau - 11.6)$ at $s = s_2^* = .255$

Although species 1 has a lower mobility than species 2, it has a larger concentration increase as is indicated by the larger slope of 2.48. For the particular parameters choosen species 1 is able to move through the bed to its accumulation position at s_1^* faster than species 2 is able to move to its accumulation position at s_2^*.

CONCLUSIONS

An accumulation criterion has been developed assuming isothermal one dimensional flow in a column. In addition it was assumed that the current was carried primarily by the small buffer species that can penetrate the particle phase

freely. Axial dispersion and mass transfer resistance were neglected. Electioneutrality was assumed for the bulk fluid and electroosmosis was neglected. A linear distribution was assumed between the bulk fluid and particle pores. The accumulation criterion, given by equation (26), gives an upper and lower limit for the operating parameter $|\mu|$. The upper and lower limits of the criterion are functions of the bed and particle porosities and the ratio of the mobility in the gel to that in free solution. The experimental data from this study could be fit to the criterion. The resulting values of the mobilities in free solution compared favorably with literature mobilities for the three proteins studied.

In order to account for unsteady state accumulation within the CACE process the theoretical model was extended by making a mass balance over a region of width Δs^*. For the case where the interface between the two packing types was very sharp this averaging region was defined to be very small, i.e. .001, and it was set equal to the region, $s_1 - s_0$, over which the proportion of polyacrylamide gel to total gel varied from 1 to 0. The model equations outside of the region Δs^* were solved using the method of characteristics. The general equations were developed for the case where the variation of the proportion of polyacrylamide gel to agarose gel could occur over any length in the column. This was useful in considering multicomponent separations where several proteins may be accumulated at different positions in the column.

The solutions to the equations where the transition from polyacrylamide to agarose was very sharp were able to predict unsteady-state accumulation and to show the effect of $|\mu|$.

For an initially loaded bed it would be desirable to start with $|\mu|$ near 1.0 and to decrease it to 0.38 (near the lower limit for accumulation) as time increased in order to always have the maximum concentration. If the bed was initially empty it would be desirable to start with $|\mu|$ near ε. The solution for the initially loaded case approaches the solution for the initially empty case at large dimensionless times. However, the initially empty case has a lag time where no protein accumulates at the interface until the protein has moved from the entrance to the interface. For the initially loaded case accumulation begins as soon as the field is applied. Thus, it would be of advantage to run the system with the bed initially loaded with protein. This would allow one to load the column using a high flow rate until a uniform concentration throughout was achieved, and thereafter the field could be turned on and the flow rate lowered to give accumulation.

If a continuous withdrawal was made at the zone of accumulation a critical value of $|\mu|$ was identified where steady state operation was achieved most rapidly. Design curves indicate that the larger steady-state concentrations can be achieved when the length of the inlet section of the bed is made smaller relative to the length of the outlet section of the bed. These steady-state concentrations are achieved at smaller $|\mu|$ (i.e. larger flow rates) and it takes larger times to reach steady state because of the material coming from the downstream side of the bed. This would indicate that it may be more desirable to operate with an initially empty bed, contrary to the afore mentioned conclusion for the case without sidestream withdrawal. Larger withdrawal rates reduce the steady-state concentration, and in some cases they may lead to a reduction in the concentration relative to the inlet concentration.

The operation of the system in the continuous mode may result in high purity of product since all the other proteins that are not accumulated will go out of the side stream with a concentration equal to their inlet concentration while the accumulated protein may have up to three orders of magnitude increase. In order to get a possibly larger product purity it would be necessary to operate semicontinuously, whereby after protein is accumulated, the column is washed of all undesirable proteins with clean buffer. The field can be turned off, and the desired pure protein washed out. Indeed, it may be easier to operate the system in the latter semicontinuous mode because withdrawal from the interface at the very low flow rates used in the process may be very difficult to control.

Adsorption is seen to not affect the accumulation criterion. It does reduce the rate of concentration increase for the transient problem. For the continuous removal problem adsorption gives an initially lower rate of concentration increase, however the concentration rises to a higher value and thereafter drops to the same steady-state concentration as the no adsorption case. The reason adsorption does not help is that the protein does not migrate when it is adsorbed to the packing. It was observed in our experiments that adsorbed protein made it easier to see the protein in the column, although it did not appear to affect the accumulation criterion.

It should also be noted that axial dispersion and mass transfer will not affect the accumulation criterion, however they will change the magnitude of the concentration and rates of concentration increase.

Analysis of the multicomponent separation gives the range of parameters that will allow more than one component to accumulate within the column. the

parameter space shows that a variation in $|\mu_1|$ by changing the current or potential with time may lead to an accumulation of unwanted species. If more than one species is shown to accumulate within the column the resolution between these species will depend upon how the column is packed. If the column is packed so that there is a sharp transition between 100% polyacrylamide and 100% agarose all proteins that accumulate will accumulate in the small averaging region at this interface. However, it may be possible to pack the column so that the variation of porosity occurs over the entire length of the column. For this case it is possible that several different proteins will accumulate at different positions in the column. The resolution between these accumulated proteins is given by equation 70. If the distance given by this equation is large enough so that diffusional spreading does not cause the proteins to overlap, the proteins would be fully separation.

The theory indicates that shorter columns will be more practical both from the standpoint of increasing the applied field per unit length of the column and shortening the time to reach steady-state. However, practical considerations of field and flow uniformities and mass transfer resistance decree larger columns. Practical operation also dictates that larger flow rates should be strived for since very low flow rates are difficult to control and have low recovery rates. However, low flow rates are necessary since the mobilities of the proteins are very low and the gel packing used in the present study has flow limitatons. Of course materials with higher mobilities (i.e. molecules other than proteins) may be more suitable for separation in this process since higher flow rates can be used to counteract the mobility. However, if the mobilities are too high the assumption that the current is carried primarily by the buffer ions may no longer be valid and the complete multicomponent equations would need to be solved.

ACKNOWLEDGEMENT

We would like to thank the North Carolina Biotechnology Center for supporting this research.

NOMENCLATURE

a, A	-	Column cross sectional area
c	-	molar fluid concentration
C	-	dimensionless fluid concentration
F	-	Faraday's constant
g	-	function in equation 43

h - function in equation 44
I - current
J* - molar diffusive flux
$\langle J_\beta^* \rangle$ - phase averaged molar diffusive flux
k - mass transfer coefficient
K - average adsorption constant, equation 20
K' - average adsorption constant, equation 17
L - bed length between electrode connections
m - molar transport rate in equations 2 and 4
M - total number of species
n - moles in fluid of particle per volume of particle, equation 13
n - unit normal from particles to fluid phase
N' - moles adsorbed per volume of fluid, equation 14
N - moles adsorbed per unit volume of particle, equation 15
q - rate of heat generation
Q - dimensionless volumetric flow rate removed from column, equation 48
Q_R - volumetric flow removed from column, equation 47
R - electrical resistance
s - dimensionless bed distance
Δs - bed distance over which particle properties change
Δs^* - size of the averaging region to determine protein concentration
t - time
u - species mobility
v - interstitial velocity = $\langle v_\beta \rangle^\beta$
V - averaging volume, equation 2
x - axial distance
z - charge on protein

Greek Symbols

α - $\beta'(1-\varepsilon)/\varepsilon$
β - internal porosity for a specific packing type
β' - average internal porosity, equation 16
δ - constants defined in equations 50 to 55
ε - bed porosity
κ - specific adsorption constant

λ - volume of a specific type of gel particle per total volume of particles, equations 16, 17, 19

μ - ratio of electrical migration to convective flow of bed, equation 20

ω - characteristic parameter, equation 23

Ω - solution conductivity

Φ' - ratio of mobility in gel to that in free solution, equation 19

ϕ - ratio of mobility in gel to that in free solution for a specific gel type

Ψ - field potential

σ - surface charge on packing, equation 8

τ - dimensionless time

τ_0^* - time given by equation 39

τ_1^* - time given by equation 40

Subscripts

β - bulk fluid phase

σ - solid particle phase

i - species index

0 - acrylamide particles

1 - agarose particles

k - specific species

REFERENCES

1. P.H. O'Farrell, Scinece, 227, 1586 (1985).

2. P.H. O'Farrell, Method of Isotope Enrichment, United States Patent 4, 290, 855 (1981).

3. P.H. O'Farrell, Method and Apparatus For Dynamic Equilibrium Electrophoresis, United States Patent 4, 323, 439 (1982).

4. R.A. Mosher, W. Thorman, N.B. Egen, P. Couasnon, and P.W. Sammens, in "New Directions in Electrophoretic Methods", ACS Symposium Series 335, J.W. Jorgenson and M. Phillips, eds., American Chemical Society, Washington DC, 1987, p. 247.

5. P.T. Noble, Biotechnol. Prog., 1, 237 (1985).

6. C.F. Ivory, W.A. Gobie, J.B. Beckwith, R. Hergenrother and M. Malc, Science, 238, 58 (1987).

7. B.J. McCoy, AIChE J., 32, 1570 (1986).

8. C.F. Ivory, Continuous Counteracting Chromatographic Electrophoresis, paper number 1064, presented at the 1987 Annual Meeting of the AIChE, New York City, Nov. 15-20 (1987).

9. J.B. Hunter, An Isotachophoretic Model of CACE, to be published in Sep. Sci. and Technol., 1988.

10. R.G. Carbonell and S. Whitaker, in "Proc. NATO Advanced Study Institute on Mechanics of Fluids in Porous Media", J. Bear and Y. Corapcioglu, eds., Martinus Nijhoff, Amsterdam, 1983, p. 121.

11. J. Newman, "Electrochemical Systems", Prentice-Hall, Englewood Cliffs, NJ, 1973.

12. T. Jovin, Ann. N.Y. Acad. Sci., 209, 477 (1973).

13. R.H. Perry and C.H. Chilton, "Chemical Engineer's Handbook", McGraw-Hill, New York, 1973.

14. C.J.O.R. Morris, Protides Biol. Fluids, 14, 543 (1966).

15. D. Rodbard and A. Chrambach, Proc. Natl. Acad. Sci., 65, 970 (1970).

16. H.-K. Rhee, R. Aris, and N.R. Amundson, "First Order Partial Differential Equations: Volume I, Theory and Application of Single Equations", Prentice Hall, Englewood Cliffs, NJ, 1986.

17. A.L. Lehninger, "Biochemistry", 2nd Ed., Worth Publishers, Inc., New York, 1975.

18. D. Rodbard, and A. Chrambach, Anal. Biochem., 40, 95 (1971).

19. P. Masson and J. Anguille, J. Chromatog., 192, 402 (1980).

20. A.R. Fanelli and E. Antonini, Biochem. Biophys. Acta, 30, 608 (1958).

21. G.H. Barlow and E. Margoliash, J. Biol. Chem., 241, 1473 (1966).

22. Biorad Chemical Division, Product Literature, 1414 Harbor Way, S. Richmond, CA, 1986.

23. B.J. Herrin, S.G. Shafer, J. Van Alstine, J.M. Harris, R.S. Snyder, J. Colloid Interface Sci., 115, 46 (1987).

24. I. Nozad, R.G. Carbonell, S. Whitaker, Chem. Engr. Sci., 40, 843 (1985).

APPENDIX A

The average flux expression for component i in the fluid phase, equation (3), and its analogous version used in the solid phase, utilize effective mobilities $u_{i\beta}$ and $u_{i\sigma}$ in the fluid and solid phases respectively. These mobilities should not be confused with the mobility of ion i in solution and the mobility of ion i in a pure gel made up of the particle material. In fact, as is shown in this appexdix, $u_{i\beta}$ and $u_{i\sigma}$ are effective mobilities that take into account the geometry of the packing and thus include the effects of the tortuosity of the path for the migration of the ion on the flux. The flux equation (3) arises from two assumptions which are valid for the particular situation found in CACE. The first is that small ions are not excluded from the particles, and the second is that the buffer ions are primarily responsible for carrying the current through the fluid and solid phases. To see how the flux equation (3) can be derived we begin with the point equations for solute transport in the fluid and solid phases

$$\frac{\partial c_{i\sigma}}{\partial t} = \nabla \cdot \{ D_{i\sigma} \nabla c_{i\sigma} + z_i F \hat{u}_{i\sigma} c_{i\sigma} \nabla \psi_\sigma \} \quad \text{in} \quad V_\sigma \tag{A-1}$$

$$\frac{\partial c_{i\beta}}{\partial t} + \nabla \cdot c_{i\beta} v_\beta = \nabla \cdot \{ D_{i\beta} \nabla c_{i\beta} + z_i F c_{i\beta} \hat{u}_{i\beta} \nabla \psi_\beta \} \quad \text{in} \quad V_\beta \tag{A-2}$$

Here $\hat{u}_{i\beta}$ and $\hat{u}_{i\sigma}$ are the true mobilities of the ions in the solution and inside the particles, and ψ_β and ψ_σ are the electrostatic potentials in each phase.

If there is no ion exclusion at the fluid-particle interface we write

$$\psi_\beta = \psi_\sigma \quad \text{on} \quad A_{\beta\sigma} \tag{A-3}$$

and

$$k_\beta \mathbf{n} \cdot \nabla \psi_\beta = k_\sigma \mathbf{n} \cdot \nabla \psi_\sigma \quad \text{on} \quad A_{\beta\sigma} \tag{A-4}$$

In these equations k_β and k_σ are electrical permittivities of the solid and fluid phases respectively.

Using the method of spatial averaging[10], one can write the averaged forms of the continuity equations as

$$\varepsilon_\sigma \frac{\partial \langle c_{i\sigma} \rangle^\sigma}{\partial t} = - \nabla \cdot \langle J^*_{i\sigma} \rangle + m_{i\beta\sigma} \tag{A-5}$$

$$\varepsilon_\beta \frac{\partial \langle c_{i\beta} \rangle^\beta}{\partial t} + \nabla \cdot \varepsilon_\beta \langle c_{i\beta} \rangle^\beta \langle v_\beta \rangle^\beta = - \nabla \cdot \langle J^*_{i\beta} \rangle - m_{i\beta\sigma} \tag{A-6}$$

where $m_{i\beta\sigma}$ is the last integral in equation (2). The average fluxes $\langle J_{i\sigma}{}^* \rangle$ and $\langle J_{i\beta}{}^* \rangle$ can be written in terms of spatial deviations between the point values of the concentration and potential,

$$c_{i\alpha} = \langle c_{i\alpha} \rangle^\alpha + \tilde{c}_{i\alpha} \qquad \alpha = \beta, \sigma \tag{A-7}$$

$$\psi_\alpha = \langle \psi_\alpha \rangle^\alpha + \tilde{\psi}_\alpha \qquad \alpha = \beta, \sigma \tag{A-8}$$

These flux expressions then take the form

$$- \langle J^*_{i\alpha} \rangle = \varepsilon_\alpha D_{i\alpha} \nabla \langle c_{i\alpha} \rangle^\alpha + \frac{1}{V} \int_{A_{\beta\sigma}} \mathbf{n}_\alpha \tilde{c}_{i\alpha} \, dA \tag{A-9}$$

$$+ \varepsilon_\alpha z_i F \hat{u}_{i\alpha} \langle \tilde{c}_{i\alpha} \nabla \tilde{\psi}_\alpha \rangle^\alpha + \varepsilon_\alpha z_i F \hat{u}_{i\alpha} \langle c_{i\alpha} \rangle^\alpha \nabla \langle \psi_\alpha \rangle^\alpha$$

$$+ z_i F \hat{u}_{i\alpha} \langle c_{i\alpha} \rangle^\alpha \frac{1}{V} \int_{A_{\beta\sigma}} \mathbf{n}_\alpha \tilde{\psi}_\alpha \, dA \quad \text{for} \quad \alpha = \beta, \sigma$$

Here $\mathbf{n}_\alpha$ is a unit normal pointing from the α phase into the other phase. For simplicity we concentrate on the electrical contribution to the flux expressions. The key is to relate the spatial deviations $\tilde{c}_{i\alpha}$ and $\tilde{\psi}_\alpha$ to the average values of the concentrations and potentials $\langle c_\alpha \rangle^\alpha$ and $\langle \psi_\alpha \rangle^\alpha$.

The electrostatic potential in the fluid external and internal to the particles can be described by the Poisson-Boltzmann equation

$$\nabla^2 \psi_\alpha = -\frac{1}{k_\alpha} \sum_i z_i F c_{i\alpha} \qquad \alpha = \beta, \sigma \tag{A-10}$$

Taking the spatial average of this equation, using the definition of the spatial deviation and subtracting the result from the point equation one obtains

$$\nabla^2 \tilde{\psi}_\alpha = -\frac{1}{V} \int_{A_{\beta\sigma}} \mathbf{n}_\alpha \cdot \nabla \tilde{\psi}_\alpha \, dA \qquad \alpha = \beta, \sigma \tag{A-11}$$

Here we have used the electroneutrality condition for the ions in the fluid and solid phases. Boundary conditions (A-3) and (A-4), together with the assumption that $\langle \psi_\beta \rangle^\beta = \langle \psi_\sigma \rangle^\sigma = \langle \psi \rangle$ leads to

$$\mathbf{n} \cdot \nabla \tilde{\psi}_\sigma - \mathbf{n} \cdot \nabla \tilde{\psi}_\beta \left(\frac{k_\beta}{k_\sigma} \right) = \mathbf{n} \cdot \nabla \langle \psi \rangle \left[\frac{k_\beta}{k_\sigma} - 1 \right] \quad \text{on} \quad A_{\beta\sigma} \tag{A-12}$$

$$\tilde{\psi}_\beta = \tilde{\psi}_\sigma \qquad \text{on} \quad A_{\beta\sigma} \tag{A-13}$$

This last assumption again relies on no exclusion of current-carrying ions. Equations (A-11) and (A-12) are completely analogous to the heat conduction problem solved by Nozad et al.[24] A solution for the closure scheme was found in the form

$$\tilde{\psi}_\alpha = \mathbf{f}_\alpha \cdot \nabla \langle \psi \rangle , \tag{A-14}$$

where $\mathbf{f}_\alpha$ is a function of position and $\nabla \langle \psi \rangle$ is nearly constant over the dimensions of a few particle diameters.

Since the spatial deviations in the concentration are usually much smaller than the average values[24], the electrical migration contribution to the ion flux in equation (A-9) can be written, using equation (A-14), in the form

$$-\langle J^{*}_{i\alpha}\rangle = \varepsilon_{\alpha} z_i F \langle c_{i\alpha}\rangle^{\alpha} \hat{u}_{i\alpha} [\mathbf{I} + \mathbf{\tau}_{\alpha}] \cdot \nabla \langle \psi \rangle \tag{A-15}$$

where $\mathbf{I}$ is the unit tensor and $\mathbf{\tau}$ is a tortuosity factor defined as

$$\mathbf{\tau}_{\alpha} = \frac{1}{V} \int_{A_{\beta\sigma}} \mathbf{n}_{\alpha} \mathbf{f}_{\alpha} \, dA \tag{A-16}$$

For a one-dimensional problem, equation (A-15) can be written in the form of equation (3) with the effective mobility defined as

$$u_{i\beta} = \hat{u}_{i\beta} [\, 1 + (\tau_{\beta})_{xx} \,] \tag{A-17}$$

A similar relation can be written for $u_{i\sigma}$.